Molecular Diagnosis & Therapy (2026) 30:403–426
https://doi.org/10.1007/s40291-026-00839-4

REVIEW ARTICLE

Colorectal Cancer: A Landscape of New Potential Radiopharmaceuticals

Veronica Serena Cabitza[1] · Pier Cesare Capponi[2] · Irene Brusa[1] · Fabrizio Vincenzi[3] · Silvia Pasquini[3] · Katia Varani[3] · Luca Urso[3,4] · Licia Uccelli[3,4]

Received: 5 November 2025 / Accepted: 15 February 2026 / Published online: 10 March 2026
© The Author(s) 2026

Abstract

In recent years, advancements in imaging techniques have contributed to a gradual yet promising reduction in colorectal cancer-related mortality. Among these, positron emission tomography (PET), particularly in combination with computed tomography using 2-deoxy-2-[fluorine-18]fluoro-D-glucose ([^{18}F]FDG), has emerged as a valuable non-invasive diagnostic tool. However, the application of [^{18}F]FDG-PET in colorectal cancer remains limited because of the radiotracer's pharmacokinetics and metabolic characteristics. As a result, [^{18}F]FDG-PET is not routinely recommended for the initial diagnosis or staging of colorectal cancer but is primarily used for assessing treatment response and disease surveillance. Additionally, colorectal cancer imaging with [^{18}F]FDG presents challenges related to false-positive results caused by radiotracer uptake in non-malignant conditions such as inflammatory bowel disease, polyps, Crohn's disease, and colitis. This inability to reliably distinguish between benign and malignant lesions remains a significant limitation in colorectal cancer imaging. To overcome these challenges, ongoing research is focused on the development of novel radiotracers capable of improving the specificity and accuracy of PET imaging in colorectal cancer. New radiolabeled probes are being investigated, including natural molecules, inflammatory markers, and target-specific immune elements, labeled with [^{18}F], [^{68}Ga], [^{11}C], and [^{64}Cu], which have shown potential in preclinical studies. Among emerging radiopharmaceuticals for colorectal cancer, only [^{68}Ga]Ga-HNI01 and [^{68}Ga]Ga-FAPI-04 have advanced to preliminary clinical evaluation phases. Despite promising initial diagnostic performance, these investigations remain limited in scale and scope, necessitating further rigorous, large-scale clinical trials to validate efficacy and safety. All these advancements could significantly enhance colorectal cancer detection and characterization, leading to earlier diagnoses and better patient outcomes.

1 Introduction

Among gastrointestinal malignancies, colorectal cancer (CRC) represents a major health concern, ranking as the second leading cause of cancer-related deaths and the third most commonly diagnosed cancer worldwide, accounting for approximately 10% of all cancer cases [1]. Early detection is crucial, as localized CRC has a 5-year survival rate of around 91%. However, once metastasis occurs, particularly to the liver, the survival rate drops dramatically to approximately 15%. The pattern of CRC metastasis varies depending on the primary tumor site: colon cancer typically spreads first to adjacent regional and retroperitoneal lymph nodes, with occasional direct liver involvement, while rectal cancer, owing to its dense vascular network, can metastasize hematogenously to the lungs at an early stage [1]. This heterogeneity underscores the complexity of CRC diagnosis

Veronica Serena Cabitza, Pier Cesare Capponi are co-first authors.

✉ Fabrizio Vincenzi
fabrizio.vincenzi@unife.it

✉ Silvia Pasquini
silvia.pasquini@unife.it

1 Nuclear Medicine, IRCCS Azienda Ospedaliero-Universitaria di Bologna, Bologna, Italy

2 Radiopharmaceutical Chemistry Section, Azienda USL-IRCCS di Reggio Emilia, Reggio Emilia, Italy

3 Department of Translational Medicine, University of Ferrara, Via Fossato di Mortara 17-19, 44121 Ferrara, Italy

4 Nuclear Medicine Unit, Azienda Ospedaliero-Universitaria di Ferrara, Ferrara, Italy

Key Points

The use of 2-deoxy-2-[fluorine-18]fluoro-D-glucose ([^{18}F]FDG)-positron emission tomography for initial colorectal cancer diagnosis and staging is limited by suboptimal pharmacokinetics and low specificity because of false positives in benign inflammatory conditions.

Novel positron emission tomography radiotracers targeting cancer hallmarks such as fibroblast activation protein, cyclo-oxygenase-2, hypoxia, redox balance, and immune markers are expanding the molecular imaging landscape in colorectal cancer.

Several radiotracers labeled with [^{18}F], [^{68}Ga], [11C], and [^{64}Cu] are in development, but only a few (e.g., [^{68}Ga]Ga-HNI01, [^{68}Ga]Ga-FAPI-04) have reached early clinical evaluation, highlighting the need for large-scale clinical trials.

Emerging radiotracers such as [^{68}Ga]Ga-FAPI and immune-positron emission tomography probes show high potential for precision oncology in colorectal cancer, offering improved lesion detection in challenging subtypes (e.g., mucinous, desmoplastic) and enabling patient stratification, despite being in early development.

Clinical translation of new radiotracers requires standardized preclinical models, harmonized imaging protocols, and multicenter studies to ensure reproducibility and applicability.

and the challenge of detecting the disease early, which is essential for determining appropriate treatment strategies and improving patient prognosis.

In recent years, mortality rates have shown a slight but encouraging decline, largely because of the use of advanced imaging techniques such as positron emission tomography/computed tomography (PET/CT). To date, the radiopharmaceutical most used in the clinical setting for CRC imaging is 2-deoxy-2-[fluorine-18]fluoro-D-glucose ([^{18}F]FDG), which represents a widely available diagnostic tool for clinicians in monitoring tumor progression. [^{18}F]FDG PET/CT is generally employed as a second-line imaging modality. There are currently few studies evaluating the utility of [^{18}F]FDG PET/CT in the initial staging of CRC neoplasms, and to date, the scientific evidence remains insufficient to recommend its routine use in this context [2]. However, [^{18}F]FDG PET/CT provides clinically meaningful gains, particularly in suspected recurrence with normal carcinoembryonic antigen (CEA), where it can detect relapse up to 2 months earlier compared with CT alone, with a high positive predictive value of 84.6% overall, which rises to 88.8% specifically for hepatic disease [3, 4]. For distant metastasis (M) staging, [^{18}F]FDG PET/CT shows superior performance to CT (+ 28.9%, sensitivity ≈ 82%, specificity ≈ 97%) [4].

By contrast, nodal (N) staging remains suboptimal (sensitivity ≈ 43–67%), particularly in advanced Union for International Cancer Control stage III/IV, where specificity drops to 33.9%. Furthermore, [^{18}F]FDG PET/CT shows notably limited sensitivity for mucinous neoplasms, a frequent subtype of CRC. Herein, mucinous histology markedly limits [^{18}F]FDG avidity (patient-level sensitivity ≈ 59–61%), consistent with a negative correlation between [^{18}F]FDG uptake and mucin content and a positive correlation with tumor cellularity [5]. False positives occur predominantly in the bowel due to inflammatory processes or granulation tissue [6]. Therefore, the identification of new fluorinated biomarkers able to "outperform" the use of [^{18}F]FDG with improved diagnostic performance could represent an important advance in the management of CRC. Research in this area has predominantly been conducted at the preclinical level, using both in vitro and in vivo models, including established cell lines and animal models. Examples of such studies include cellular assays, cellular uptake experiments, biodistribution analyses, and imaging using MicroPET. Representative CRC cell lines, such as HCT8, SW620, LoVo, HT29, HCT116, and many others, have been widely used, along with xenograft mouse models in which human tumor tissues are implanted into immunocompromised mice.

Despite the inherent limitations of preclinical models, these studies represent an essential step forward in our understanding of CRC and may provide the foundation for future clinical development. The current challenge in CRC imaging lies in the development of novel, more specific radiotracers capable of accurately distinguishing benign from malignant lesions, thereby reducing false positives and improving diagnostic accuracy. Advancements in this field could enhance the effectiveness of PET imaging in CRC management and potentially improve patient survival through earlier and more precise diagnoses. A wide range of molecules have been investigated, and these include natural molecules, inflammatory markers, and target-specific immune elements, radiolabeled with [^{18}F], [^{68}Ga], [^{11}C], and [^{64}Cu].

In this review, we examine the current landscape of radiopharmaceutical discovery and development in the context of CRC, with a particular emphasis on preclinical research, as only a few of these promising radiotracers have progressed to clinical application. We also provide an overview of the experimental methodologies used to evaluate these compounds, highlighting the in vitro and

in vivo models adopted in the referenced studies. To ensure comparability, the data are normalized based on imaging acquisition times, and the CRC cell lines used in each study are directly compared (Table 1).

2 Review Methodology

This narrative review summarizes radiopharmaceuticals investigated for CRC imaging, with a primary focus on preclinical studies and selected early-phase clinical evidence. The literature was identified through searches of PubMed and Scopus, including articles published up to mid-2025. Original studies reporting in vitro experiments, preclinical in vivo imaging, or clinical PET imaging in CRC models or patients were considered eligible. Review articles, purely therapeutic studies, and investigations exclusively focused on non-CRC malignancies were excluded.

Data extraction was performed qualitatively, focusing on radiotracer characteristics, biological targets, radionuclides, experimental platforms, and CRC models employed (cell lines, xenografts, chemically induced models, chorioallantoic membrane (CAM) models, or clinical cohorts). Imaging outcomes were collected as reported in the original studies and included standardized uptake values (SUVs) [maximum SUV/mean SUV (SUVmax/SUVmean)], percentage injected dose per gram (%ID/g), tumor-to-background ratios (e.g., tumor-to-muscle, tumor-to-blood), and imaging timepoints.

Comparisons across studies were conducted descriptively. When multiple acquisition times were reported, imaging results were interpreted in relation to the acquisition time to allow qualitative normalization and improve comparability. Colorectal cancer cell lines and model systems were categorized and compared across studies to highlight biological and methodological variability.

3 Preclinical Studies

3.1 Fluorinated Radiopharmaceuticals for CRC

From a radiochemical perspective, the synthesis of [^{18}F]-labeled radiopharmaceuticals is generally more complex than that of metallic radiometal-based radiotracers, such as those labeled with [^{68}Ga]. [^{18}F]-labeling often involves multi-step nucleophilic or electrophilic substitution reactions, which require carefully designed precursors and, in many cases, the use of protecting groups to achieve regioselective fluorine incorporation without compromising biological activity. These procedures are essential to ensure that the fluorine atom is introduced at chemically stable positions that preserve or enhance the molecule's pharmacokinetics and target specificity. Despite the synthetic challenges, [^{18}F] remains one of the most widely used radionuclides owing to its favorable imaging characteristics, including a high positron emission yield (97%), low positron energy (Emax = 0.634 MeV; Emean = ≈ 0.25 MeV), and a half-life of 110 min.

3.1.1 [^{18}F]DFA

The 6-deoxy-6-[^{18}F] fluoro-L-ascorbic acid, abbreviated as [^{18}F]DFA (Fig. 1a), is a structural analog of ascorbic acid (AA), designed to identify tumor cells that overexpress the sodium-dependent vitamin C transporter (SVCT2) [7], which is considered a biomarker for AA-based treatment in patients with CRC. It has been reported that CRC cancer cells with high SVCT2 expression are more sensitive to AA treatment than those with low SVCT2 expression and consequently, SVCT2 has been considered a potential target for AA therapy in patients with CRC [7, 8]. He et al. performed an in vitro biological evaluation of [^{18}F]DFA, demonstrating that unlabeled AA can competitively inhibit

Table 1 Main cellular lines used in reference studies

Cell line	Cancer type	Origin
LoVo	Grade IV Dukes C colorectal cancer	Human derivation
SW620	Dukes C colorectal cancer	Human derivation
SW480	Dukes C colorectal cancer; epithelial-like morphology	Human derivation
SW1222	Dukes' C adenocarcinoma of the colon	Human derivation
HCT8	Human ileocecal adenocarcinoma	Human derivation
HCT116	Human colon cancer	Human derivation
HT29	Human colorectal adenocarcinoma grade II	Human derivation
LS174T	Dukes B colorectal cancer	Human derivation
CT26	Colon carcinoma induced in a BALB/c mouse using the carcinogen N-nitroso-N-methylurethane	Mouse derivation
MC38	Mouse colon adenocarcinoma cell line	Mouse derivation

the uptake of the [^{18}F]DFA radiotracer by CRC cells, indicating a clear selectivity for the intended target [7]. Substrate-competitive inhibition studies were conducted in the presence of structural analogs, and unlabeled AA caused a significant reduction (88–90%) in [^{18}F]DFA uptake across various CRC cell lines examined in the study. To characterize differences among the tested cell lines, the researchers conducted a Western blot analysis of HCT8 and HCT116 cells, which showed low SVCT2 expression, in contrast to SW620, SW480, and LoVo cells, which exhibited higher SVCT2 levels. The experimental results indicated a correlation between SVCT2 expression and radiotracer accumulation. However, this correlation was not observed uniformly across all tested cell lines, suggesting only relative selectivity. Notably, although SW620 cells expressed the highest levels of the transporter, they did not exhibit the greatest radiotracer uptake, implying the possible involvement of alternative mechanisms of [^{18}F]DFA internalization or efflux. Nevertheless, the authors considered the panel of cell lines used to be representative of CRC models and reported an overall good correlation between SVCT2 expression and [^{18}F]DFA uptake (Fig. 1b) [7]. The in vivo results obtained from mice bearing implanted tumors were promising, although only two tumor models were used. Both SW620 and HCT8 cell lines were implanted in the same mouse, and in both cases, the radiotracer showed uptake and retention, confirming the in vitro findings. As expected, because of the molecule's hydrophilicity and its structural similarity to AA, it exhibited high distribution in the adrenal glands, kidneys, intestines, and liver. MicroPET images (Fig. 1c) in tumor-bearing mouse models and tissue biodistribution confirmed a predominant visceral retention, along with radiotracer accumulation in both implanted tumors, SW620 and HCT8, the latter exhibiting the lowest SVCT2 expression in vitro. The MicroPET images obtained were of acceptable quality; although the spatial resolution was not optimal, the implanted tumors were clearly identifiable, indicating a certain degree of selectivity for SVCT-expressing tissues. The biodistribution of [^{18}F]DFA was evaluated in mice bearing CRC xenografts to assess its potential as a PET imaging agent. The radiotracer demonstrated a favorable distribution, with significant uptake in highly perfused organs, suggesting a combination of excretory pathways and potential affinity for metabolically active tissues. Notably, [^{18}F]DFA was also successfully taken up by tumor tissues, with higher accumulation observed in SW620 xenografts compared with HCT8, along with a clear time-dependent increase in uptake.

This trend was further reflected in improved tumor-to-background ratios, particularly in relation to muscle and blood, supporting the radiotracer's ability to effectively differentiate tumor tissue. Although uptake was modest compared with traditional radiotracers, the capacity

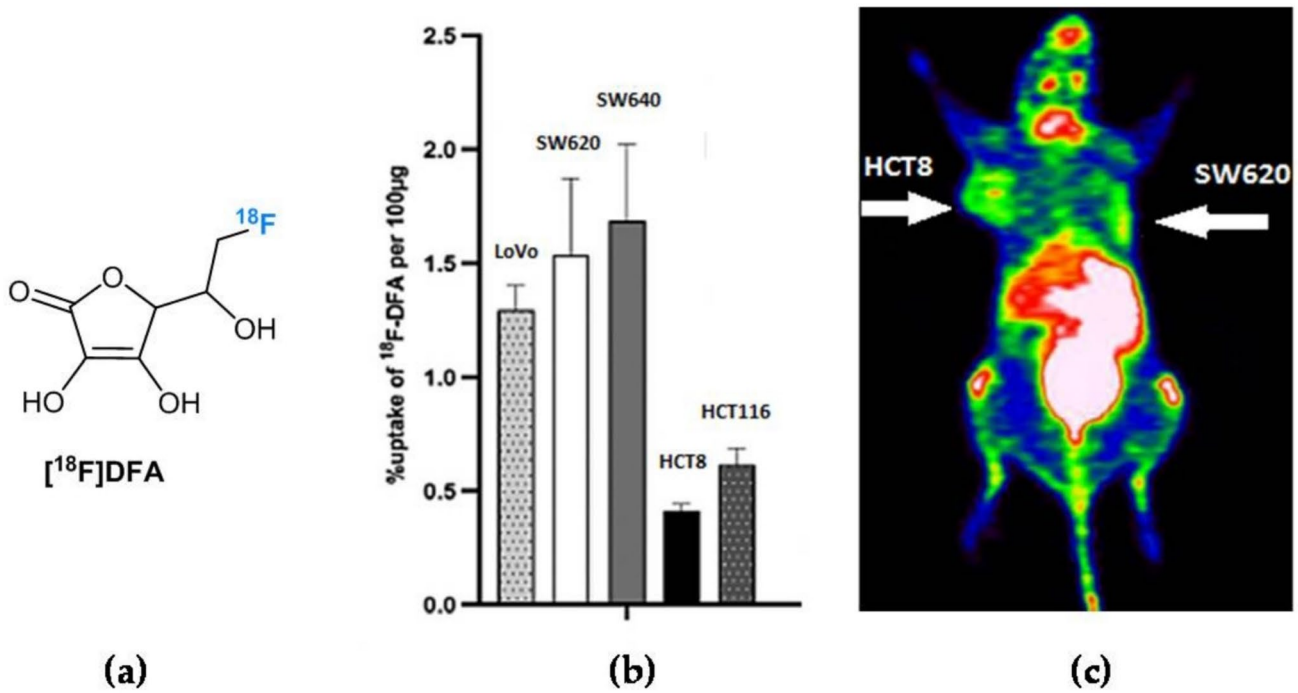


Fig. 1 In vitro and in vivo results with 6-deoxy-6-[^{18}F] fluoro-L-ascorbic acid ([^{18}F]DFA): **a** chemical structure of [^{18}F]DFA; **b** uptake of [^{18}F]DFA in the cellular lines considered at 30 min. Data are shown as mean ± standard deviation; **c** in vivo uptake of [^{18}F]DFA in HCT8 and SW620 cell lines. Arrows indicate the uptake of [^{18}F]DFA in tumor tissues, 60 min after injection [7]

of [^{18}F]DFA to distinguish between different tumor types adds value to its diagnostic potential. The tissue distribution data, expressed as % ID/g (mean ± standard deviation, 5 mice per timepoint), revealed the following trend: SW620 tumor (1.14 ± 0.27 at 30 min, 1.39 ± 0.37 at 60 min) and HCT8 tumor (0.70 ± 0.33 at 30 min, 1.05 ± 0.17 at 60 min). These results are consistent with the in vitro data and validate the radiotracer retention observed in the animal model. Taken together, the data obtained from CRC models, both in vitro and in vivo, are promising. Given the limited availability of imaging agents for CRC, [^{18}F]DFA emerges as a potentially valuable candidate for further research, offering favorable radiopharmacological properties and supporting its future clinical application or use in studies on ascorbic acid (AA) metabolism.

3.1.2 [^{18}F]FMISO

[^{18}F]Fluoromisonidazole ([^{18}F]FMISO) [Fig. 2a] is a well-known and widely used radiopharmaceutical for evaluating and quantifying hypoxia levels in tumors. Because of its lipophilic nature, [^{18}F]FMISO is able to effectively distribute and diffuse into viable cells, where the nitro group of the nitroimidazole moiety is reduced. In non-hypoxic cells, the reduced molecule can be re-oxidized in the presence of oxygen and subsequently diffuses out of the cell, ultimately being eliminated. In contrast, in rapidly proliferating tumor cells where oxygen concentrations are typically ≤ 10 mmHg, oxidation of the nitro group does not occur. As a result, [^{18}F]FMISO accumulates within the cells, enabling its quantitative visualization. Although [^{18}F]FMISO has been applied clinically in a variety of tumors, to the best of our knowledge, the only reported example of its preclinical application in CRC was provided by Zhang et al. [9]. The authors investigated the biological behavior of CRC by exploring the uptake of [^{18}F]FMISO both in vitro and in vivo. Three CRC cell lines were employed as experimental models: LoVo, HT29, and HCT116, which were incubated under hypoxic conditions to mimic the tumor microenvironment and used both in in vitro assays and in vivo xenograft models. In the in vitro experiments, the cellular uptake of [^{18}F]FMISO was evaluated over time (Fig. 2b) for each cell line. At 30 min, no statistically significant differences were observed among the lines. However, at 60, 120, and 240 min, LoVo cells demonstrated a significantly higher uptake compared with both HT29 and HCT116 cells and overall, all cell lines exhibited time-dependent accumulation. It is important to note that different cell lines may exhibit significant variability in radiotracer uptake over time and the use of a broad panel of cellular models is crucial to account for phenotypic heterogeneity and to ensure more reliable and generalizable results. While in vitro experiments offer valuable preliminary insights into binding affinity and specificity, only in vivo imaging can conclusively demonstrate the radiopharmaceutical's tropism for tumor tissue. To strengthen their experimental findings, Zhang et al. further

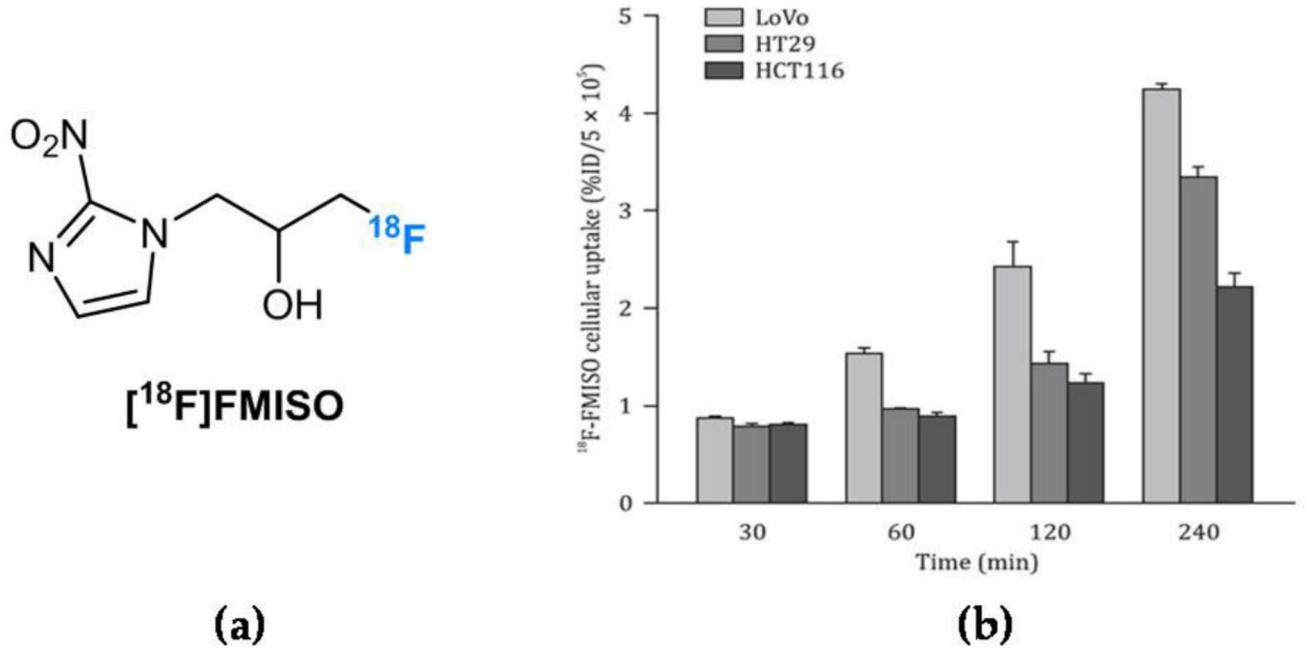


Fig. 2 In vitro results with [^{18}F]FMISO. **a** Chemical structure of the [^{18}F]FMISO; **b** the quantitative histogram of [^{18}F]FMISO cellular uptake. Cells were incubated with [^{18}F]FMISO for 30, 60, 120, and 240 min (min), respectively. The percentage of the injected dose (% ID) of [^{18}F]FMISO per 5 × 10^5 cells. Data are expressed as the mean ± standard deviation [9]

complemented the imaging data with immunohistochemical analysis of hypoxia biomarkers, providing additional evidence of radiotracer localization in biologically relevant tumor microenvironments [9]. This integrative approach not only reinforces the specificity of the radiotracer but also highlights its potential role in detecting functionally aggressive tumor regions, which may be relevant for prognosis and therapy planning. The researchers performed PET imaging 4 h after an [^{18}F]FMISO injection, which corresponded to the timepoint of maximum uptake observed in vitro. The MicroPET images (Fig. 3) obtained were of good quality, and in the CRC mouse models (LoVo, HT29, and HCT116), varying levels of uptake were observed, expressed as SUV-max, which correlated well with the cellular uptake in vitro. The results showed the following trend: LoVo tumor: 1.97 ± 0.15 > HT29 tumor: 1.72 ± 0.12 >HCT116 tumor: 1.55 ± 0.09. The researchers also highlighted a significant correlation between the uptake of [^{18}F]FMISO and the expression of hypoxic biomarkers such as HIF-1α and GLUT-1, further reinforcing the link between tumor hypoxia and the radiotracer's accumulation. This correlation was particularly evident in different CRC cell lines used, with increasing hypoxia factor levels observed (LoVo > HT29 > HCT116) and where LoVo cells showed the highest expression of hypoxia factors. These results indicate that LoVo cells, derived from a stage IV Dukes type C colon adenocarcinoma, exhibit the most pronounced hypoxic response to [^{18}F]FMISO both in vitro and in vivo. This suggests that the LoVo cell line may provide an excellent model for studying tumor hypoxia and assessing the effectiveness of hypoxia-targeted therapies. Furthermore, the study underscores the potential for [^{18}F]FMISO to be used as an imaging tool to differentiate between CRC cell lines with varying degrees of hypoxia, reflecting their distinct biological characteristics. Such capabilities could be particularly valuable for in vivo imaging, allowing for the identification and monitoring of tumor regions with low oxygen levels. This differential uptake between cell lines may enable a more personalized approach to treatment by targeting the specific metabolic and hypoxic profiles of tumors. As a gold-standard hypoxia radiotracer, [^{18}F]FMISO has already shown promising applications in clinical settings for other tumor types, such as head and neck squamous cell carcinoma, glioblastoma and other high-grade gliomas, non-small-cell lung cancer, esophageal cancer, pancreatic cancer, and soft-tissue sarcomas [10–15]. However, in the context of CRC, clinical evidence remains limited, largely confined to small heterogeneous investigational studies without standardized acquisition protocols or validated quantitative thresholds, so routine use is not currently recommended [16].

3.1.3 [^{18}F]AlF-NOTA-A6P

The overexpression of specific proteins represents a strategic approach for the targeted imaging of cancer cells. In the case of CRC, integrin-α6, a subtype of the integrin family involved in tumor cell adhesion, invasion, and migration, has emerged as a promising molecular target. Integrins are

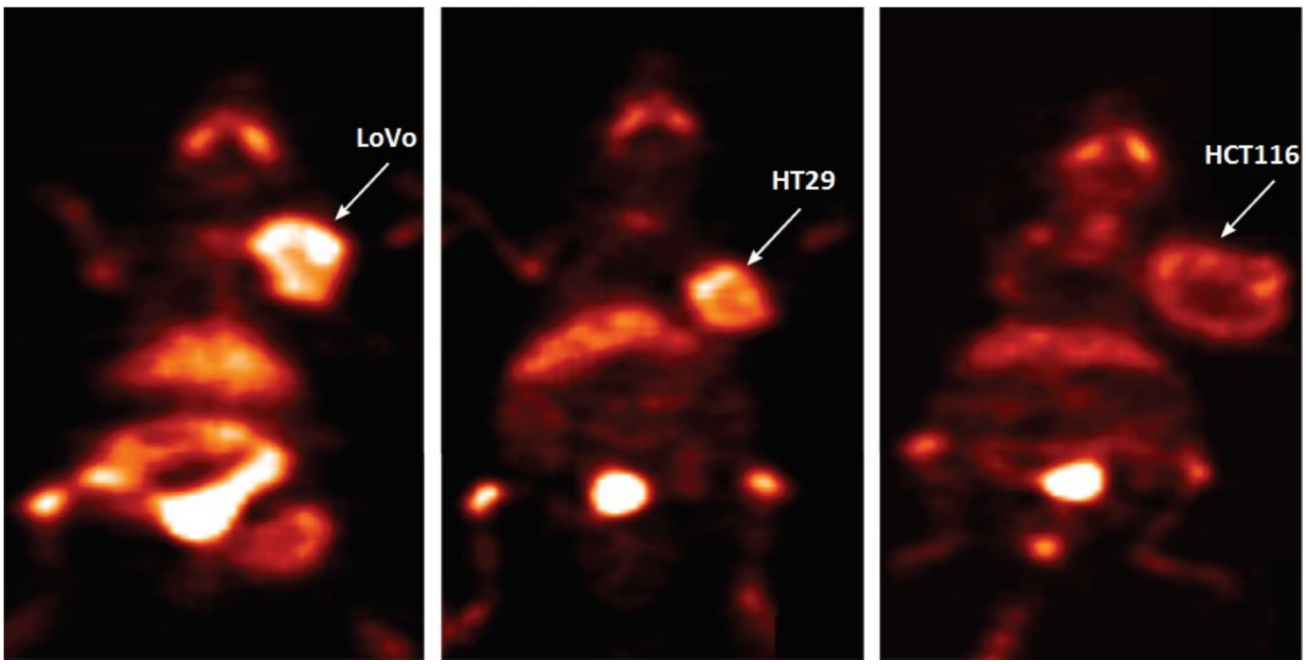


Fig. 3 Arrows indicate the uptake of [^{18}F]FMISO in tumor (LoVo, HT29, and HCT116) tissues, 240 min after injection [9]

a transmembrane glycoprotein family that mediate interactions between cells and the extracellular matrix, and they play a central role in processes such as signal transduction, cellular motility, and survival. Notably, integrin-α6 is overexpressed in several malignancies, including CRC, while its expression is low or negligible in most normal tissues [17]. This differential expression pattern makes integrin-α6 a particularly attractive biomarker for the development of targeted PET radiotracers. In this context, a novel peptide-based radiotracer, [^{18}F]AlF-NOTA-A6P, has been developed to target integrin-α6 (Fig. 4a) [18]. The radiotracer is based on a modified A6P peptide, engineered through cyclization and site-specific amino acid substitutions to enhance its pharmacokinetic stability and binding affinity. The peptide is conjugated to the chelator 1,4,7-triazacyclononane-1,4,7-triacetic acid (NOTA) via a polyethylene glycol (PEG) linker, which improves aqueous solubility and reduces non-specific interactions. Radiolabeling is achieved through an aluminum-fluoride complexation strategy (Al^{18}F), in which the fluorine-18 is efficiently incorporated into the NOTA chelator. This method allows for straightforward labeling under mild conditions and leverages the favorable imaging characteristics of [^{18}F], including its suitable half-life and excellent resolution. Peptides have long been recognized as valuable vectors in radiopharmaceutical research because of their ease of synthesis, structural versatility, and compatibility with a wide array of radionuclides. Their low immunogenicity and cost effectiveness further contribute to their utility in molecular imaging applications. In the study conducted by Chen et al. [18], [^{18}F]AlF-NOTA-A6P underwent a thorough chemical and biological evaluation. Initial assessments confirmed the radiotracer's hydrophilicity and high stability in human serum. Western blot analyses were then performed to identify CRC cell lines with differing levels of integrin-α6 expression. In this case, the researchers used three human cell lines as a study model: the LS174T, HT29 and SW620. LS174T and HT29 cells exhibited high integrin-α6 expression, while SW620 cells showed minimal expression. These cell lines were used for in vitro binding assays and for generating xenograft models in immunocompromised mice. MicroPET/CT imaging revealed that [^{18}F]AlF-NOTA-A6P accumulated significantly more in LS174T tumors than in SW620 tumors (Fig. 4b), confirming the radiotracer's selectivity for integrin-α6 positive tissues. Tumor uptake was rapid and sustained, with a clearly favorable tumor-to-muscle ratio, suggesting high in vivo stability and efficient tumor targeting. Specificity was further validated through a blocking study conducted in HT29 tumor-bearing mice (Fig. 4c), where co-injection of an excess of unlabeled NOTA-A6P significantly reduced radiotracer uptake. A quantitative analysis showed that the tumor-to-muscle ratio in blocked animals was approximately half

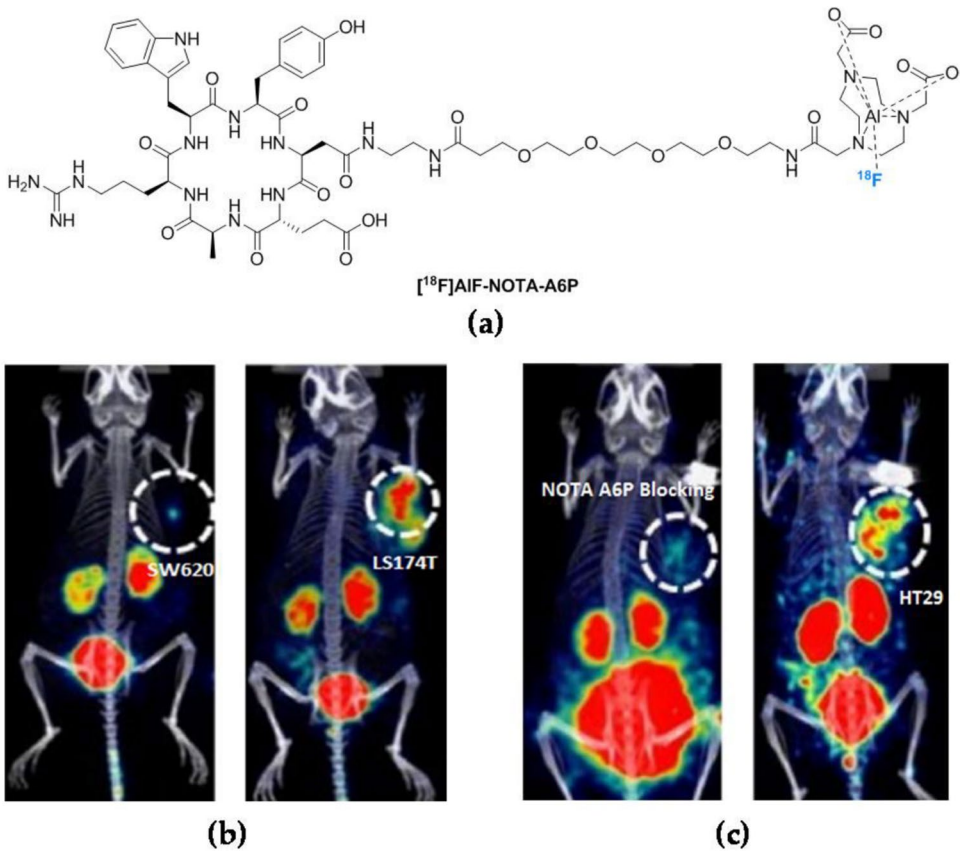


Fig. 4 In vivo results with [^{18}F]AlF-NOTA-A6P: **a** chemical structure of [^{18}F]AlF-NOTA-A6P; **b** dynamic MicroPET images of implanted tumors SW620 and LS174T; 60 min after injection; **c** blocking study conducted in HT29 tumor-bearing mice; left, co-injection of an excess of unlabeled NOTA-A6P significantly reduced radiotracer uptake [18]

that of unblocked controls at 60 min post-injection. Once again, it becomes evident that the choice of cell line and its phenotypic characterization are critical factors that directly influence imaging outcomes. Integrating cellular analysis techniques such as immunohistochemistry, Western blotting, and others is essential to understand the biological features of each model used and to reinforce the scientific rationale of the study. Overall, preclinical data suggest that [^{18}F]AlF-NOTA-A6P is a promising PET imaging agent for the detection of integrin-α6 overexpressing tumors, including CRC. Its high specificity, confirmed by blocking studies, stability, and a good imaging contrast, make it a possible candidate for further investigation.

3.1.4 [^{18}F]FB-IL-2

Another radiotracer, developed on CRC models and designed for imaging immune activity, is N-(4-[^{18}F]fluorobenzoyl)-interleukin-2 ([^{18}F]FB-IL-2) [Fig. 5a], obtained by conjugating interleukin (IL)-2 with a previously labeled [^{18}F] fluorinated succinimidyl ester [19]. Interleukin-2 is a 15.3-kDa monomeric glycoprotein, also known as a lymphokine, that binds with high affinity to surface receptors (IL-2 receptor), which are prominently expressed in activated T lymphocytes. The use of radiotracers based on immune elements takes advantage of the induction of specific receptors following immune activation, a phenomenon that also involves the tumor microenvironment and can be used to identify new therapeutic and diagnostic targets in tumors, including CRC. In vitro studies conducted by Khanapur et al. confirmed the binding affinity and specificity of [^{18}F]FB-IL-2 for the IL-2 receptor, through receptor saturation experiments on activated peripheral blood mononuclear cells, followed by in vivo experiments in mice [19]. Cellular activation was achieved by adding phytohemagglutinin, followed by incubation of the cells with [^{18}F]FB-IL-2 at 37°C for 30 min. A significant difference in radiotracer binding was observed between non-activated and activated peripheral blood mononuclear cells (Fig. 5b). To evaluate binding specificity, the cells were pre-incubated with an excess of recombinant IL-2 protein (20 ng/mL) to saturate the IL-2 receptors, which resulted in an approximately three-fold reduction in [^{18}F]FB-IL-2 binding. After confirming the binding specificity, the researchers employed murine cell lines modeled for CRC in the in vivo imaging experiments. Dynamic PET imaging, followed by ex vivo biodistribution studies, showed that the radiotracer has a kinetic profile and tissue distribution similar to that of native IL-2, with predominant renal excretion. In murine models with MC38 and CT26 colon tumors, a significantly higher radiotracer uptake was observed in MC38 tumors compared with CT26 (Fig. 5c), which can be attributed to the immunogenic phenotype of the MC38 tumors. Imaging also revealed minimal brain uptake, confirming that the protein cannot cross the blood–brain barrier, low bone uptake (ex vivo biodistribution), and no defluorination in vivo, essentially confirming a favorable pharmacokinetic profile for a potential radiopharmaceutical. Overall, [^{18}F]FB-IL-2 proved to be a valuable tool for discriminating between two murine tumor lines with different immunological profiles, suggesting its potential use in studying immune activity linked to CRC. These preclinical studies were primarily conducted on murine models, and further developments can be expected by testing its imaging capability on human CRC cell lines.

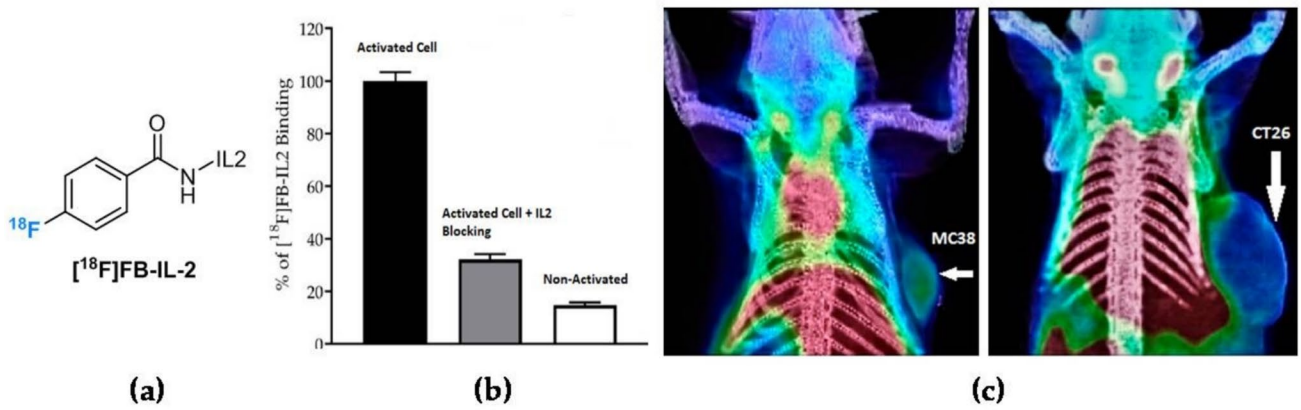


Fig. 5 In vitro and in vivo results with N-(4-[^{18}F]fluorobenzoyl)-interleukin-2([^{18}F]FB-IL-2): **a** chemical structure of [^{18}F]FB-IL-2; **b** in vitro binding assessment of [^{18}F]FB-IL-2 in mouse peripheral blood mononuclear cells. The binding was shown to be specific by a significant reduction in the binding of [^{18}F]FB-IL-2 when pre-treated with excess non-radioactive recombinant IL-2. Data are expressed as the mean ± standard deviation; **c** dynamic MicroPET images of implanted tumors SW620 and LS174T, 60 min after injection (1.65 ± 0.24 MC38 vs 1.21 ± 0.03 CT26, percentage injected dose per gram) [19]

3.2 Potential Radiopharmaceuticals for CRC Labeled with Gallium-68

In recent years, CRC research has focused on new approaches for imaging and early diagnosis with innovative PET radiotracers based on the radionuclide Gallium-68 [^{68}Ga]. Gallium-68 is a positron-emitting radionuclide with a physical half-life of 67.7 min and an average positron energy of approximately 0.83 MeV, higher than that of fluorine-18 ([^{18}F], ~ 0.25 MeV). As a result, [^{68}Ga] exhibits a longer positron range in tissue, which can slightly reduce spatial resolution in PET imaging compared with [^{18}F]. Nevertheless, [^{68}Ga] emits positrons with high efficiency, with around 89% of its decays proceeding via β^+ emission, making it highly suitable for PET applications. Moreover, it is conveniently available through a [^{68}Ge]/[^{68}Ga] generator system, eliminating the need for an on-site cyclotron and enabling flexible decentralized radiopharmaceutical production. Chemically, [^{68}Ga] forms stable complexes with bifunctional chelators such as DOTA, NOTA, and HBED, which can be conjugated to a variety of biomolecular vectors, including peptides and small molecules. These features make [^{68}Ga] a powerful alternative to [^{18}F], especially in the context of personalized oncology, preclinical development, and theranostic strategies. Among the radiopharmaceuticals currently under investigation, a number of [^{68}Ga]-labeled agents have shown promising results for precision PET imaging in CRC, supporting improved lesion detection and patient stratification in both preclinical and clinical studies. This section summarizes the most relevant recent evidence, focusing on newly developed radiotracers, emerging biological targets, and innovative strategies that are expanding the diagnostic landscape of CRC.

3.2.1 [^{68}Ga]Ga-DOTA-C21

Orteca et al. explored the potential of a novel [^{68}Ga]-labeled radiotracer [^{68}Ga]Ga-DOTA-C21 (Fig. 6a), based on curcumin, a well-known natural molecule with anti-tumor properties, for early detection of CRC using PET imaging [20]. In contrast with the first generation of [^{68}Ga]-labeled curcumin complexes, which suffered from low stability and rapid degradation, [^{68}Ga]Ga-DOTA-C21 showed increased stability in physiological conditions [20, 21]. The new DOTA derivative of curcumin was evaluated for cell uptake, internalization, and efflux in HT29 colon-rectal cancer cells, demonstrating strong tumor-targeting properties mediated by its curcumin structure. However, in mice bearing HT29 xenografts, [^{68}Ga]Ga-DOTA-C21exhibited not only significant accumulation in the tumor, with a tumor-to-muscle ratio that increased over time, but also accumulation in on-target organs, especially in the liver and intestine (Fig. 6b) [20]. Therefore, given the limited specificity, modifications are necessary to improve tumor uptake.

3.2.2 [^{68}Ga]Ga-GSH

Another promising pathway targeted for CRC imaging is glutathione (GSH) metabolism, which is often altered in tumor cells and has been shown to play a key role in cancer progression and drug resistance. Hence, Sidiq et al. investigated the radiosynthesis and characterization of a [^{68}Ga]-labeled glutathione dimer ([^{68}Ga]Ga-GSH), for its

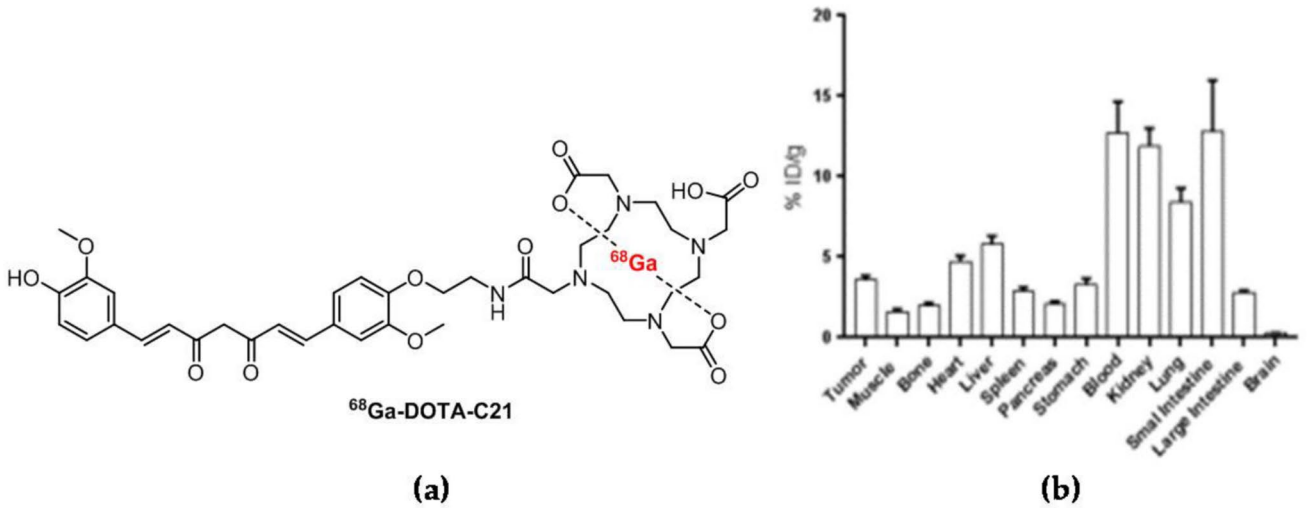


Fig. 6 Chemical structure and in vivo evaluation of [^{68}Ga]Ga-labeled DOTA-C21: **a** chemical structure of [^{68}Ga]Ga-DOTA-C21; **b** biodistribution in multiple organs of [^{68}Ga]Ga-DOTA-C21 in HT-29 colorectal cancer bearing nude mice (n = 5, mean ± standard deviation) at 90 min post intravenous injection [20]. *%ID/g* percentage injected dose per gram

application in imaging diagnostics of colon cancer in murine models [22]. For this purpose, 24 male Sprague Dawley rats were used, with half serving as controls and the other 12 induced with colon cancer via subcutaneous injections of dimethylhydrazine. [^{68}Ga]Ga-GSH demonstrated a higher uptake at the tumor site compared with healthy tissue, peaking at 90 min post-administration, along with a high uptake in the bladder and kidneys, consistent with its excretion pathway. Additionally, an increasing tumor-to-normal colon [^{68}Ga]Ga-GSH uptake ratio was observed over time, which is potentially linked to the elevated expression of gamma-glutamyltransferase, a key enzyme in glutathione metabolism that may predict drug resistance [22].

3.2.3 [^{68}Ga]Ga-DOTA.SA.FAPi

The fibroblast activation protein (FAP) is a serine protease widely expressed in the stroma of many cancer cells, including CRC. In recent years, FAP has garnered increasing attention in the field of radiopharmaceutical research as a promising target of cancer imaging and therapy [23–26]. Fibroblast activation protein inhibitor 04 (FAPI-04) PET/CT has been evaluated across multiple CRC settings, including primary staging, restaging, and detection of recurrence. In brief, FAPI PET/CT often outperforms [^{18}F]FDG PET/CT for peritoneal and nodal disease and is particularly useful in low-FDG-avid histologies (mucinous and signet ring), where its high tumor-to-background contrast can refine staging and influence management [27–30]. Limitations include heterogeneous FAP expression across primary and metastatic sites, non-tumor uptake in inflammation or post-treatment changes that can yield false positives, and lower sensitivity for osseous metastases compared with [^{18}F]FDG [31]. Overall, FAPI PET/CT is a valuable adjunct best interpreted in a multidisciplinary context rather than a full replacement for conventional imaging. Subsequent research has increasingly focused on next-generation FAPI-04 analogs engineered for improved pharmacokinetics, tumor retention, and image contrast. For this reason, Moon et al. developed a novel PET radiotracer targeting FAP, [^{68}Ga]Ga-DOTA.SA.FAPi (Fig. 7a), based on the FAP inhibitor UAMC1110 pharmacophore and using squaric acid as a linker between the quinoline moiety and the DOTA chelator [32]. The introduction of the squaramide (squaric acid) linker simplifies chemical synthesis, as squaric acid chemistry facilitates coupling to both the chelator and the targeting vector without the need for protecting groups, owing to its selectivity for primary amines. This circumvents the requirement for complex synthetic pathways. Moreover, the use of squaric acid as a linker unit has been shown to exert a positive impact on the pharmacological properties of the final products, enhancing in vitro binding affinity as well as in vivo and ex vivo performance.

In a murine xenograft model of human CRC HT-29, [^{68}Ga]Ga-DOTA.SA.FAPi demonstrated significant tumor accumulation at 1-h post-injection, with high tumor-to-blood, tumor-to-colon, and tumor-to-muscle ratios (Fig. 7b). The authors' results showed that the highest radiotracer uptake occurred in the tumor, enabling a high contrast in PET imaging, while marked accumulation in the bladder reflected predominant elimination of the radiotracer via the urinary route [32]. These findings highlight the potential of [^{68}Ga]Ga-DOTA.SA.FAPi as

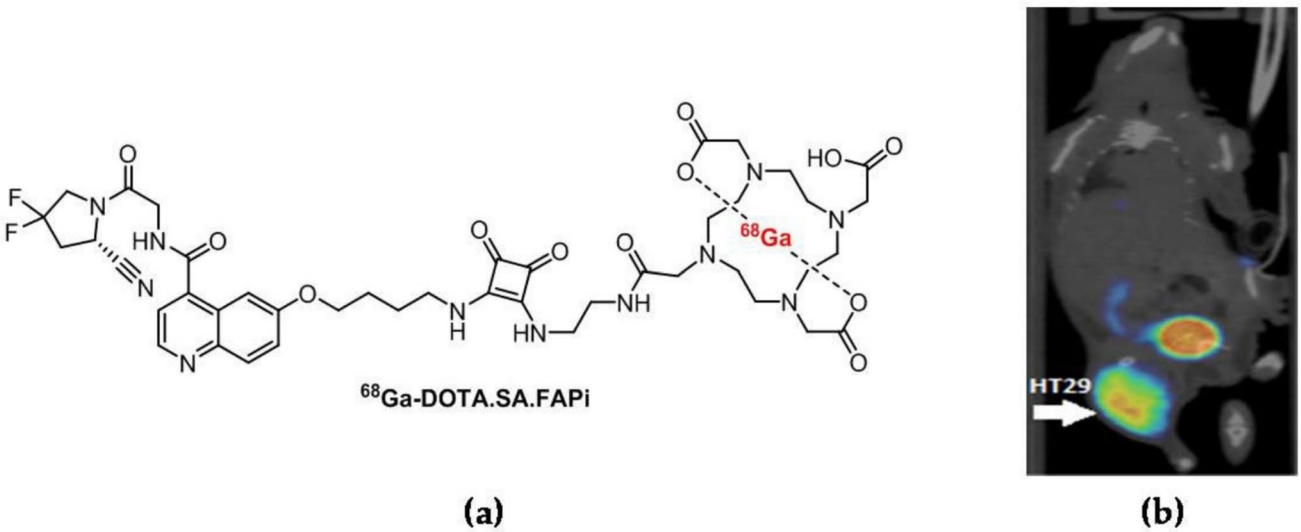


Fig. 7 Chemical structures and in vivo evaluation of [^{68}Ga]Ga-labeled DOTA.SA.FAPi: **a** structure of [^{68}Ga]Ga-DOTA.SA.FAPi; **b** representative coronal PET/CT image (MIP) of an HT-29 xenograft mouse 60 min after injection of [^{68}Ga]Ga-DOTA.SA.FAPi [32]

an encouraging tool for the imaging of FAP-expressing tumors.

3.2.4 [^{68}Ga]Ga-Pentixafor

In the context of CRC, overexpression of the chemokine receptor CXCR4 has been strongly correlated with metastatic spread and tumor progression. Accordingly, CXCR4-targeted radiotracers offer a promising strategy for the non-invasive imaging and localization of CXCR4-expressing malignant cells. Benčurová et al. were the first to evaluate [^{68}Ga]Ga-Pentixafor (Fig. 8a) as a new CXCR4-targeting radiotracer for CRC imaging [33]. The authors studied two human CRC cell lines, one CXCR4-positive (HT29) and one CXCR4-negative (HCT116). While [^{18}F]FDG accumulated similarly in both cell lines, HT29 cells demonstrated significantly higher [^{68}Ga]Ga-Pentixafor binding and internalization capabilities compared with HCT116 cells. Here, specific CXCR4 binding was confirmed by a reduction in [^{68}Ga]Ga-Pentixafor uptake when a CXCR4 antagonist was co-administered (Fig. 8b). Conversely, the binding of [^{68}Ga]Ga-Pentixafor to HCT116 cells was low and non-specific. This difference was also reflected in in vivo studies using a CAM xenograft model, where [^{68}Ga]Ga-Pentixafor uptake was significantly higher in tumors derived from HT29 cells compared with those derived from HCT116 cells (Fig. 8c). These results were further confirmed by a reduction in radiotracer accumulation after CXCR4 receptor blocking [33].

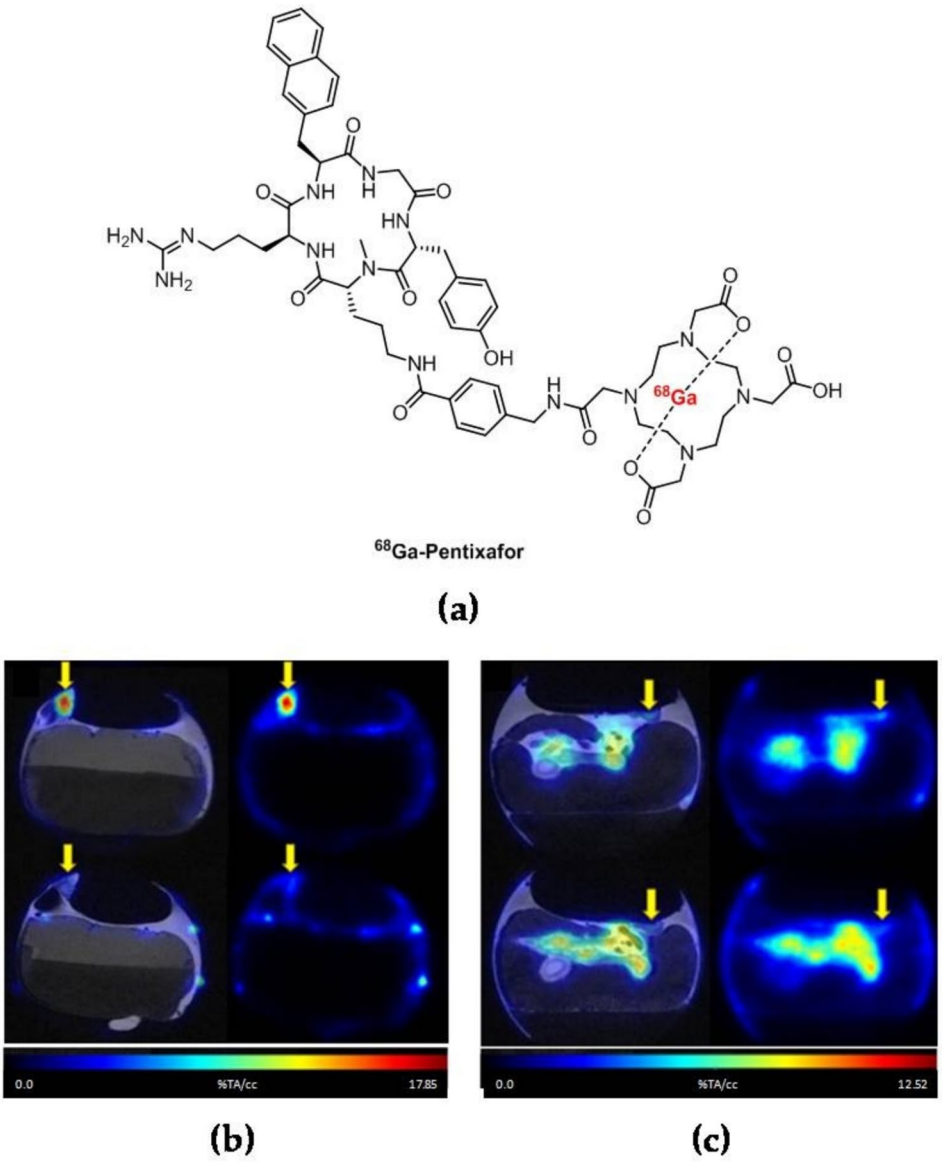


Fig. 8 Chemical structure of [^{68}Ga]Ga-labeled Pentixafor and representative images of [^{68}Ga]Ga-Pentixafor PET/MRI in the HT29 CAM-xenograft model: **a** structure of [^{68}Ga]Ga-Pentixafor; **b** upper row: baseline scan after intravenous injection of [^{68}Ga]Ga-Pentixafor in HT29 CAM-xenograft model. Lower row: blocking of [^{68}Ga]Ga-Pentixafor uptake in the same mouse on the following day; (**c**) upper row: baseline scan after intravenous injection of [^{68}Ga]Ga-Pentixafor in HCT116 CAM-xenograft model. Lower row: blocking of [^{68}Ga]Ga-Pentixafor uptake in the same mouse on the following day [33]

3.2.5 [^{68}Ga]Ga-ES-02

Although a limited number of studies have investigated the expression and prognostic significance of human epidermal growth factor receptor (HER) family members in patients with colon cancer, Zhang et al. recently developed two novel peptides intended for PET imaging of HER-2-positive CRC, namely [^{68}Ga]Ga-ES-01 and [^{68}Ga]Ga-ES-02 (Fig. 9a) [34–37]. In HT-29 HER2-positive tumor cells, both peptides demonstrated specific tumor uptake, which significantly decreased in the presence of an excess of unlabeled peptides, confirming the specificity of HER-2 binding (Fig. 9b). Notably, HER-2 binding affinity assays showed higher binding affinity of the cyclic peptide [^{68}Ga]Ga-ES-02 (Kd = 24.29 ± 4.95 nM) compared with [^{68}Ga]Ga-ES-01 (Kd = 30.44 ± 4.55 nM). In terms of stability, [^{68}Ga]Ga-ES-02 exhibited superior performance both in vitro and in vivo when compared to [^{68}Ga]Ga-ES-01. In HT29 tumor-bearing mice, PET imaging studies further supported the enhanced properties of [^{68}Ga]Ga-ES-02, which showed greater tumor uptake and background contrast compared with the linear peptide [^{68}Ga]Ga-ES-01, with maximal SUVmax and SUVmean values at 30 min post-injection (Fig. 9c) [37]. Overall, [^{68}Ga]Ga-ES-02 emerges as a promising candidate for targeted PET imaging of HER-2-positive CRC, owing to its higher binding affinity, enhanced stability, and superior imaging characteristics.

3.2.6 [^{68}Ga]Ga-DN68

Recently, a novel and promising target has been identified in oncologic imaging: Nectin-4. Nectin-4 is a cell adhesion protein that is overexpressed in several solid malignancies, making it an attractive candidate for targeted therapies such

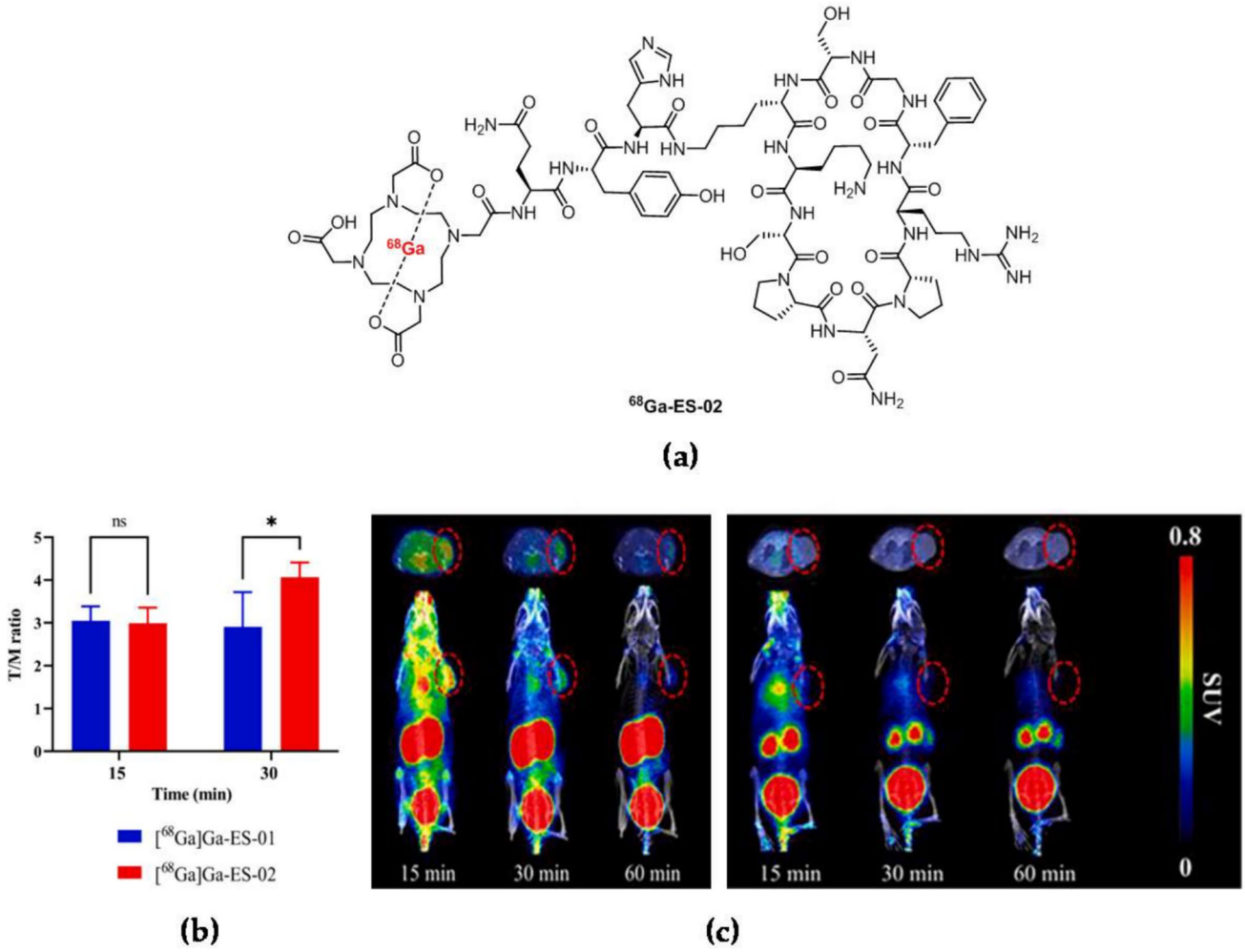


Fig. 9 Chemical structure of the human epidermal growth factor receptor 2-targeting cyclic peptide [^{68}Ga]Ga-ES-02 and in vivo studies in HT29-tumor bearing mice: **a** structure of [^{68}Ga]Ga-ES-02; **b** tumor/muscle ratio of [^{68}Ga]Ga-ES-01 and [^{68}Ga]Ga-ES-02 in HT-29 tumor-bearing mice at 15 and 30 minutes (min) after injection; **c** representative fused positron emission tomography/computed tomography images after injection of [^{68}Ga]Ga-ES-02 (left) with experimental group and (right) blocking group [37]

as antibody–drug conjugates and for molecular imaging applications [38]. It should be noted that Nectin-4-targeted approaches are currently under active evaluation in other tumor entities, where they have reached more advanced stages of translational and clinical development. However, in the specific context of metastatic CRC, its use has thus far been limited to preclinical models, with overall unsatisfactory outcomes. A study analyzing 251 tumor specimens from patients with metastatic CRC reported that Nectin-4 expression was predominantly low, with only 5% of samples exhibiting high expression levels [39]. Nevertheless, Ge et al. developed a novel PET radiotracer, [^{68}Ga]Ga-DN68, designed for Nectin-4 imaging [40]. This study employed the MC38-Nectin-4 tumor model, where MC38 represents a murine colon adenocarcinoma cell line. The findings demonstrated that [^{68}Ga]Ga-DN68 accumulated specifically in MC38-Nectin-4 tumors, enabling rapid tumor visualization (within 30 min) and yielding a high tumor-to-background ratio, thereby allowing clear delineation of lesions [40]. Despite these promising technical results in preclinical colon cancer models, the clinical translation of Nectin-4 imaging in metastatic CRC remains limited by the generally low expression of this target in the majority of patients [38, 40].

3.3 Potential Radiopharmaceuticals for CRC Labeled with Non-Standard Isotopes

Recent advancements in CRC diagnostics have also dealt with the development of innovative radiotracers labeled with non-standard radionuclides to enhance molecular imaging capabilities. While Gallium-68 and Fluorine-18 remain the mainstay, other radionuclides, including Carbon-11 and Copper-64, have been investigated in selected settings for their unique properties.

3.3.1 [^{11}C]MC1

Carbon-11's short half-life ($t_{1/2}$ = 20.38 min) allows for high-resolution imaging with minimal background interference, making it ideal for targeting biomarkers linked to inflammation and various cancer hallmarks such as cyclooxygenase 2 (COX-2) [41, 42]. Indeed, COX-2 overexpression is associated with poor prognosis and cancer progression, making it a promising target for CRC imaging and early detection [42, 43]. Boyle et al. explored the potential of repurposing 6-methoxy-2-(4-(methylsulfonyl)phenyl)-*N*-(thiophen2-ylmethyl)pyrimidin-4-amine ([^{11}C]MC1, Fig. 10a), a potent and selective COX-2-targeted radiopharmaceutical for clinical neuro-PET research (NCT04396873, NCT04582916), for rapid translation to patients with cancer [44]. For that, two rodent models of CRC, ICRscid mice with COX-2 positive HT-29 and COX-2 negative HCT-116

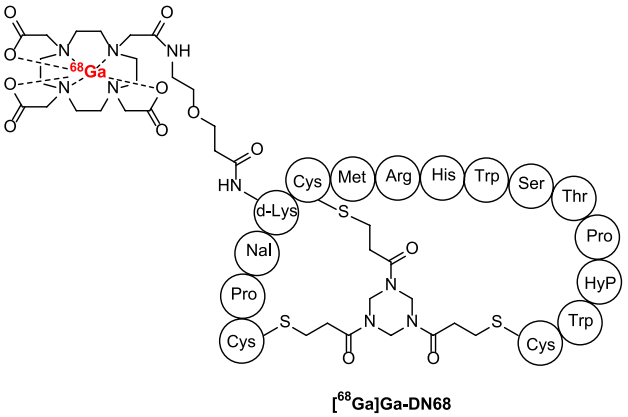


Fig. 10 Chemical structure of [^{68}Ga]Ga-DN68

CRC xenografts were used. [^{11}C]MC1 demonstrated to selectively accumulate in COX-2-positive tumors, with high tumor-to-muscle ratios (3.94, 60 min post injection) and significant reductions in uptake following pre-treatment with COX-2 inhibitors (Fig. 11b). Conversely, COX-2 negative HCT-116 tumor xenografts were not visualized following injection of [^{11}C]MC1. [^{11}C]MC1 also exhibited excellent metabolic stability, with over 90% of the compound remaining intact in tumor tissue at 40 min post injection, based on a radiometabolic analysis.

3.3.2 [^{64}Cu]-Tz-NOTA and [^{64}Cu]-Tz-SarAr

Copper-64, with its favorable half-life ($t_{1/2}$ = 12.7 h) and chelation chemistry with a variety of chelators, is a versatile radioisotope suitable for both PET imaging and the development of pre-targeted radiopharmaceuticals. Briefly, pre-targeting strategies rely on the design of an antibody that can bind both a target antigen and a radiolabeled hapten. First, the antibody is injected into the blood, slowly accumulates in the tumor, and concomitantly clears from the blood. After this localization interval, a radiolabeled hapten is administered intravenously. This radioligand is designed to selectively bind through an in vivo click chemistry reaction to the antibody, followed by the rapid clearance of its excess thanks to its small size. In essence, the final radioimmunoconjugates formed at the tumor itself (Fig. 12) [45–47]. In 2013, the group of Zeglis et al. reported the development of a pre-targeted system for CRC PET imaging based on the bioorthogonal inverse electron demand Diels-Alder (IEDDA) reaction between tetrazine (Tz) and trans-cyclooctene (TCO) moieties [48]. This system included two components: (1) a CRC-targeting huA33 antibody (huA33-TCO) that targets the A33 antigen found in over 95% of colorectal carcinomas, covalently modified with transcyclooctene and (2) a NOTA-modified tetrazine radiolabeled with [^{64}Cu] ([^{64}Cu]-Tz-NOTA, Fig. 13a). In A33-antigen

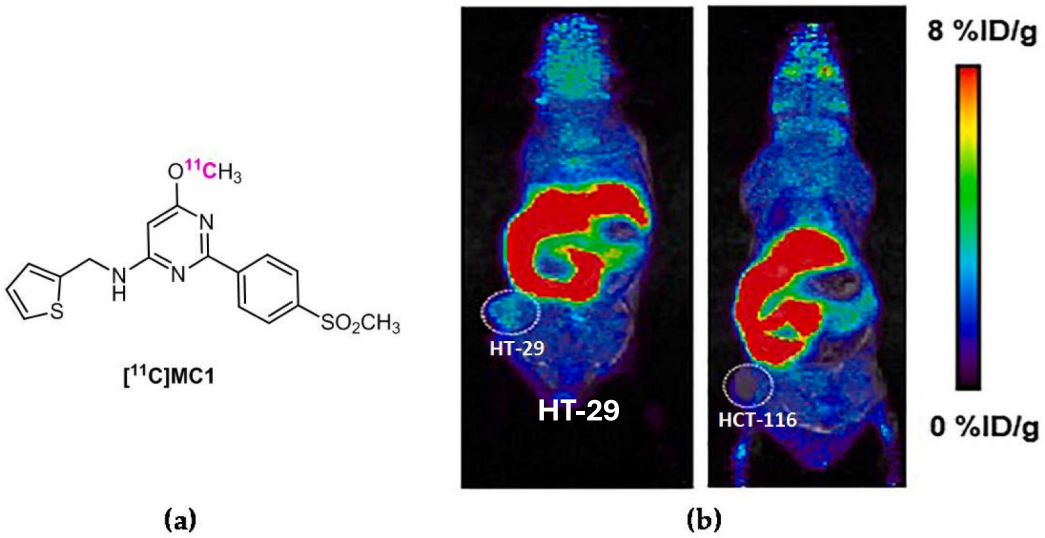


Fig. 11 Structure of the [^{11}C]-labeled COX-2 radiotracer [^{11}C]MC1 (**a**) and dynamic positron emission tomography/magnetic resonance imaging of [11C]MC1 in HT-29 CRC and in HCT-116 CRC xenograft mice at baseline (**b**) [44]. *%ID/g* percentage injected dose per gram

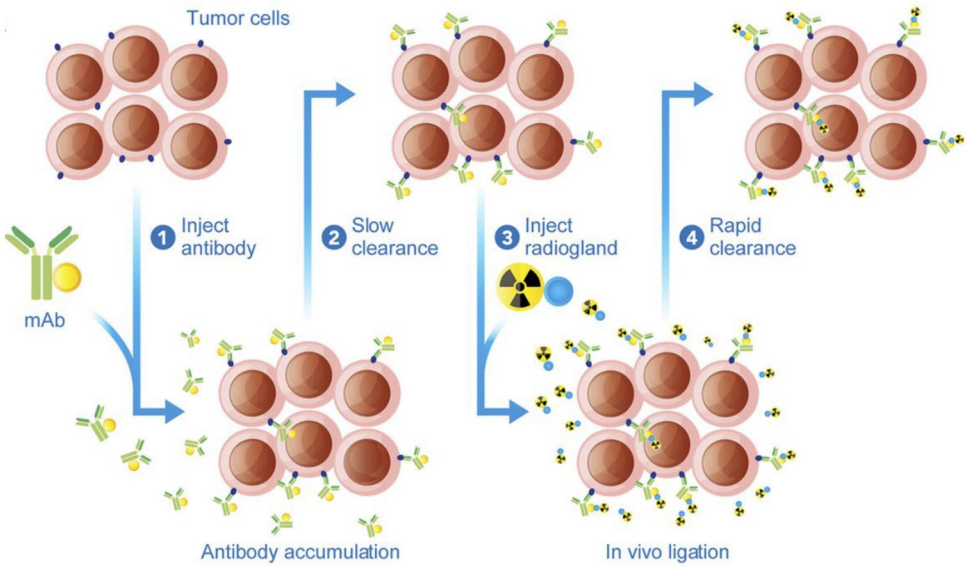


Fig. 12 Schematic of the pre-targeted positron emission tomography imaging strategy. *mAB* monoclonal antibody

expressing SW1222 hCRC xenografts pre-treated with A33-TCO, [^{64}Cu]-Tz-NOTA construct was efficiently taken up by the SW1222 tumor, with excellent delineation from background by 12 h after injection (Fig. 13b) [48]. A comparison with the preassembled antibody [^{64}Cu]-NOTA-A33 showed that the tumor-to-blood ratios of the antibody-based and the pre-targeting system were comparable at 24 h post-injection (2.9 ± 0.4 and 1.9 ± 0.6, respectively) [Fig. 13c]. These data clearly illustrate that the pre-targeted system might represent a qualitatively and quantitatively comparable alternative to [^{64}Cu]-based antibody imaging. However, the clinical translation of this first-generation pre-targeting strategy was hindered by the undesirable slow clearance of the radioligand through the gastrointestinal tract. Two years later, the same group synthesized two novel [^{64}Cu]-labeled tetrazine constructs bearing structural modifications designed to accelerate their clearance from the body [49]. Among them, [^{64}Cu]-Tz-SarAr (Fig. 13a) demonstrated rapid excretion solely through the renal system in healthy athymic nude mice. Because of its promising pharmacokinetic profile, [^{64}Cu]-Tz-SarAr was further assayed in mice bearing A33 antigen-expressing SW1222 human colorectal carcinoma tumors pre-treated with hA33-TCO. The combination of huA33-TCO and [^{64}Cu]-Tz-SarAr yielded specific uptake of the radiotracer in the tumor and low activity concentrations in non-target tissues (Fig. 13d). A slightly higher

activity concentration in the tumor was observed compared with the first-generation [^{64}Cu]-Tz-NOTA system; i.e., at 12 h after injection, the tumor-to-blood and tumor-to-muscle activity ratios for [^{64}Cu]-Tz-SarAr were 3.1 ± 0.8 and 45.1 ± 8.6, respectively, compared with 1.8 ± 0.5 and 26.6 ± 6.6 with [^{64}Cu]-Tz-NOTA. To further improve the pre-targeting strategy, in a subsequent study the group developed a site-specifically modified CRC-targeting huA33-trans-cyclooctene immunoconjugate (^{ss}huA33-PEG$_{12}$-TCO) [50]. Preclinical in vivo validation studies were performed in mice bearing A33 antigen-expressing SW1222 xenografts. To this end, mice were first administered ^{ss}huA33-PEG$_{12}$-TCO and, following accumulation intervals of 24 h, [^{64}Cu]-Tz-SarAr. Positron emission tomography imaging and biodistribution results clearly showed how the use of the better defined and homogeneous ^{ss}huA33-PEG$_{12}$-TCO construct in combination with [^{64}Cu]-Tz-SarAr could delineate tumor tissue as early as 1-hour post-injection with excellent tumor-to-background measure (21.5 ± 5.6 at 24 h post injection) [Fig. 13e]. Together, these studies showed that this pre-targeted approach could enable a rapid and clear visualization of tumor tissue, with an improved pharmacokinetic profile compared with the first-generation strategy, and overall effective doses far below those produced by directly labeled radioimmunoconjugates. Given the novel aspects of this technology, it was licensed to Clarity under a worldwide exclusive license. A phase I clinical trial using the pre-targeted technology with [^{64}Cu]-Tz-SarAr and a trans-cyclooctene-modified humanized 5B1 immunoconjugate (hu5B1-TCO) in patients with pancreatic cancer, CRC, bladder cancer, or solid tumors with elevated CA19-9 is now open for recruitment at the Memorial Sloan Kettering Cancer Centre (NCT05737615).

4 Clinical Studies

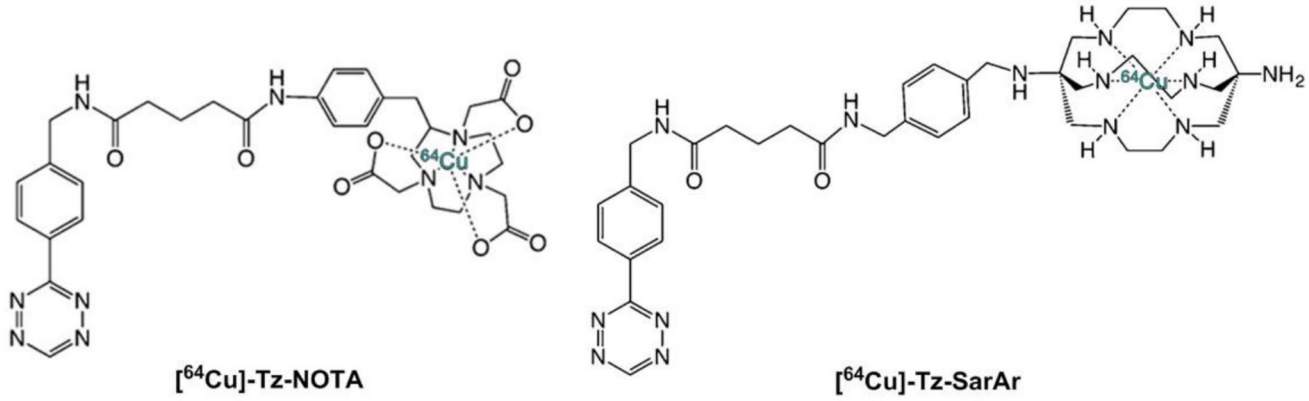
Although preclinical research on novel radiopharmaceuticals for CRC has rapidly advanced in recent years, the number of clinical studies remains limited. Most clinical investigations are still in early-phase trials or involve small patient cohorts, reflecting the initial steps of clinical translation. Nevertheless, few innovative compounds, particularly nanobody-based radiotracers and FAP-targeting agents, have begun to show promising diagnostic performance in human subjects. The following section presents two relevant examples: [^{68}Ga]Ga-HNI01, a nanobody-based radiotracer targeting CEA, and [^{68}Ga]Ga-FAPI-04, a FAP inhibitor currently being tested for its ability to distinguish malignant from benign colorectal lesions with greater precision than conventional [^{18}F]FDG PET.

4.1 [^{68}Ga]Ga-HNI01

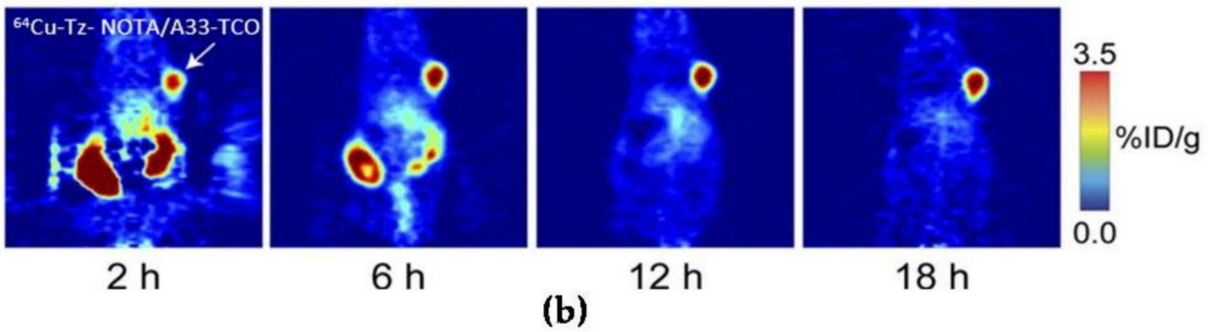
Li et.al. evaluated the efficacy of a novel [^{68}Ga]-labeled nanobody targeting CEA, namely [^{68}Ga]Ga-HNI01 [51]. The use of nanobodies derived from llama immunization with CEA proteins was driven by several advantages over traditional full-length antibodies, such as faster blood clearance and improved tissue penetration. In vitro, HNI01 specifically bound to tumor cells overexpressing CEA, such as LS174T, but not to those expressing low levels of CEA, such as HT-29, as confirmed by immunohistochemical analyses. However, no correlation was found between the tumor uptake of the radiotracer and the serum CEA level. Positron emission tomography imaging in murine models with LS174T tumors showed clear visualization of malignancies as early as 30 min after the injection of [^{68}Ga]Ga-HNI01, while uptake was inhibited by co-injection of unlabeled HNI01, confirming the specificity of CEA binding. Thanks to these promising pre-clinical results, a phase I clinical trial involving nine patients with primary and metastatic CRC was initiated. Positron emission tomography imaging with [^{68}Ga]Ga-HNI01 was able to identify different CRC lesion types in the reported cohort, including hepatic, pulmonary, and pancreatic metastases. As observed in vivo, the radiotracer showed significant accumulation in the kidneys but a low background in other organs. Notably, in some patients, an abnormal uptake was observed in healthy colorectal tissue adjacent to the tumor, which may reflect increased CEA expression and warrants further investigation. Overall, these preliminary data suggest that [^{68}Ga]Ga-HNI01 may be a useful PET radiotracer for CRC and may offer advantages over [^{18}F]FDG for the detection of small metastases in certain sites (e.g., liver, lymph nodes, and pancreas), although these findings require validation in larger cohorts. In addition, [^{68}Ga]Ga-HNI01 could support patient selection for anti-CEA therapies and may help in the assessment of gastrointestinal adverse effects [51].

4.2 [^{68}Ga]Ga-FAPI-04

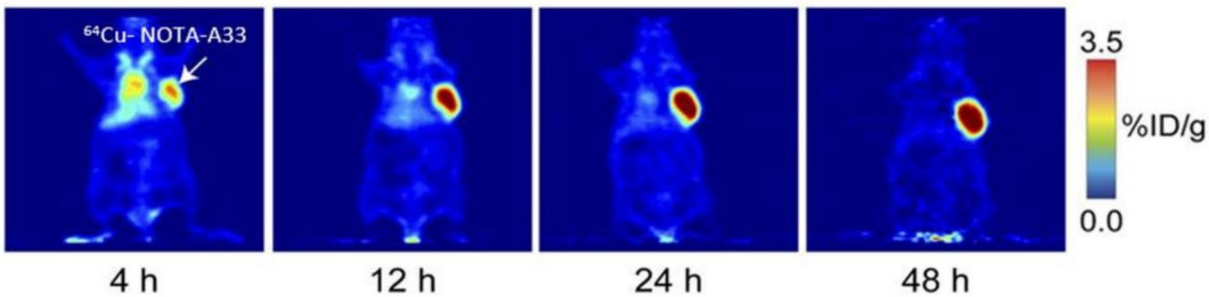
Beyond CRC, FAP-targeted radiopharmaceuticals are being investigated in other tumor entities, with some approaches already further along in clinical evaluation. In the context of CRC, Shangguan et al., building on previous studies by Pang et al. and the Kömek group, recently demonstrated the efficacy of another FAP-targeting radiopharmaceutical, [^{68}Ga]Ga-FAPI-04 (Fig. 14), in differentiating benign from malignant [^{18}F]FDG-avid colorectal lesions [29, 52–54]. The prospective clinical study (2020 CER No. 172), conducted at the Ruijin Hospital, involved 22 patients with gastric cancer and 172 additional patients were retrospectively enrolled. The published results suggest that [^{68}Ga]Ga-FAPI-04 may


[64Cu]-Tz-NOTA
[64Cu]-Tz-SarAr

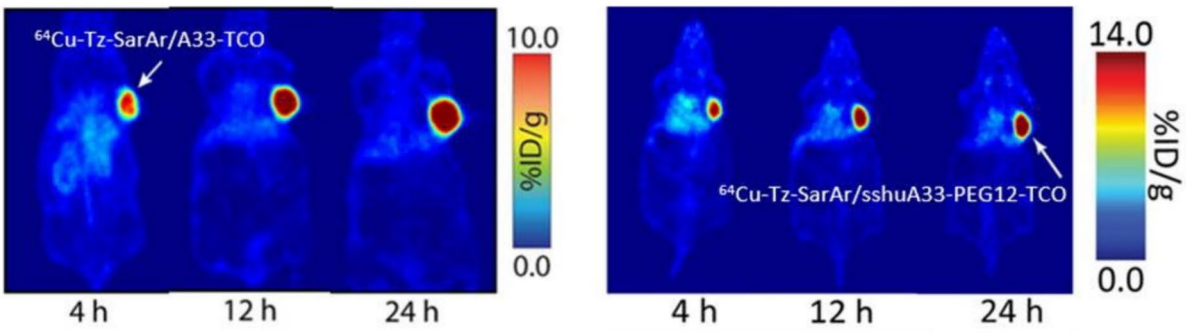
(a)


64Cu-Tz- NOTA/A33-TCO
3.5
%ID/g
0.0
2 h
6 h
12 h
18 h

(b)


64Cu- NOTA-A33
3.5
%ID/g
0.0
4 h
12 h
24 h
48 h

(c)


64Cu-Tz-SarAr/A33-TCO
10.0
%ID/g
0.0
4 h
12 h
24 h
64Cu-Tz-SarAr/sshuA33-PEG12-TCO
14.0
%ID/g
0.0
4 h
12 h
24 h

(d) (e)

◂**Fig. 13** Structures and pre-targeting PET imaging using [^{64}Cu]-Tz-Bn-NOTA/A33-TCO, [^{64}Cu]-Tz-SarAr/A33-TCO, and [^{64}Cu]-Tz-SarAr/^{ss}huA33-PEG$_{12}$-TCO in comparison to the intact antibody [^{64}Cu]-NOTA-A33: **a** chemical structures of [^{64}Cu]-Tz-Bn-NOTA and [^{64}Cu]-Tz-SarAr, **b** mice bearing subcutaneous SW1222 xenografts were administered A33-TCO. After 24 hours (h), the same mice were administered [^{64}Cu]-Tz- NOTA; **c** positron emission tomography imaging between 4 and 48 h after injection of [^{64}Cu]-NOTA-A33 in mice bearing subcutaneous SW1222 xenografts; **d** female athymic nude mice bearing subcutaneous SW1222 xenografts were administered with huA33-TCO. After an accumulation interval of 24 h, the same mice were then administered [^{64}Cu]-Tz-SarAr; **e** athymic nude mice bearing subcutaneous A33 antigen-expressing SW1222 human colorectal carcinoma xenografts were first injected with ^{ss}huA33-PEG$_{12}$-TCO. After an accumulation interval of 24 h, the same mice were then administered [^{64}Cu]-Tz-SarAr [48–50]. *%ID/g* percentage injected dose per gram

improve the differentiation of benign and malignant lesions compared with [^{18}F]FDG, both in terms of specificity and tumor-to-background contrast. Indeed, eight out of 22 patients with gastric cancer (but without CRC) showed [^{18}F]FDG uptake in the colon, whereas [^{68}Ga]Ga-FAPI-04 PET was negative at these sites, supporting the possibility that [^{18}F]FDG uptake may reflect non-malignant findings. In this cohort, among colorectal lesions with high [^{18}F]FDG avidity, 80 out of 94 (85.1%) pathologically malignant lesions were FAP positive, while only 16 out of 78 (20.5%) premalignant or benign lesions showed weak uptake of [^{68}Ga]Ga-FAPI-04. These data are consistent with higher FAP expression in malignant lesions and support further evaluation of [^{68}Ga]Ga-FAPI-04 as a diagnostic tool in this setting. Following completion of the prospective study, a new clinical trial is ongoing at the same hospital (NCT06601075), and its results will be informative for validating these findings in larger cohorts [53].

4.3 [^{11}C]-4DST

The short physical half-life of carbon-11 was further exploited to develop a novel thymidine radiotracer, 4′-[methyl-^{11}C]-thiothymidine ([^{11}C]-4DST, Fig. 15), that could incorporate into DNA as a cell proliferation marker [55, 56]. Fukuda and coworkers investigated the effectiveness of [^{11}C]-4DST PET/CT in detecting CRC, as compared to the common [^{18}F]FDG PET/CT [57]. Both radiotracers were able to detect CRC in all 18 patients of the study. However, the uptake of [^{11}C]-4DST, while weakly correlated with proliferative activity as measured by the Ki-67 index, was significantly lower than that of [^{18}F]FDG (median SUVmax for [^{11}C]-4DST was 6.02 ± 2.55 vs median SUVmax for [^{18}F]FDG was 13.91 ± 7.62). Reasonably, the authors speculated that malignant lesions are commonly rich in metabolically active and inflammatory cells while fewer cells are proliferating, leading to a greater uptake of [^{18}F]FDG relative to [^{11}C]-4DST [58].

4.4 [^{68}Ga]Ga-Trivehexin

Integrin αvβ6 is a transmembrane protein whose expression is nearly absent in healthy tissues but markedly upregulated in several epithelial malignancies, particularly pancreatic cancer, head and neck squamous cell carcinoma, and CRC. This expression profile supports αvβ6 evaluation as a target for molecular imaging [59, 60]. [^{68}Ga]Ga-Trivehexin is an innovative PET radiopharmaceutical that specifically targets integrin αvβ6. From a radiochemical standpoint, [^{68}Ga]Ga-Trivehexin represents an optimization of previous multimeric radiotracers, achieved by substituting phenylalanine residues with tyrosine to increase hydrophilicity (Fig. 16). According to preclinical and early clinical data, this modification may contribute to faster blood clearance and lower non-specific uptake, with a potentially improved tumor-to-background contrast. The trimeric design yielded up to an 18-fold increase in binding affinity for αvβ6 compared to monomeric radiotracers [59]. Although most preliminary clinical experience with [^{68}Ga]Ga-Trivehexin PET/CT has focused on pancreatic ductal adenocarcinoma and head and neck squamous cell carcinoma, in the study by Das et al. involving 32 oncology patients, one case of CRC infiltrating the pancreatic head was evaluated using [^{68}Ga]Ga-Trivehexin PET/CT. In that case, radiotracer uptake was lower (SUVmax = 3.6) than the metabolic uptake observed with [^{18}F]FDG PET (SUVmax = 5.6) [60]. Overall, further clinical studies on larger patient cohorts are warranted to refine clinical indications and validate preliminary findings.

5 Discussion

The development of novel PET radiotracers for CRC has significantly expanded in recent years, offering a diverse portfolio of molecular targets that reflect key hallmarks of cancer biology (Table 2). These include markers of inflammation (e.g., COX-2), stromal activation (e.g., FAP), hypoxia (e.g., HIF-1α), redox balance (e.g., glutathione pathways), amino acid transport, and immune system modulation. However, when comparing the studies analyzed in this review, important differences emerge in terms of experimental models, imaging endpoints, and translational applicability. Despite the promising results, most evidence derives from preclinical models that incompletely reflect the biological complexity of human CRC. Differences in the tumor microenvironment, immune contexture, and target expression across commonly used cell lines may therefore limit the direct translatability of these findings to clinical settings. Preclinical studies

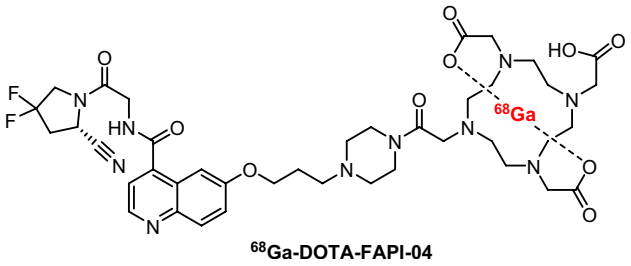


Fig. 14 Chemical structure of the fibroblast activation protein-targeting [^{68}Ga]Ga-FAPI-04

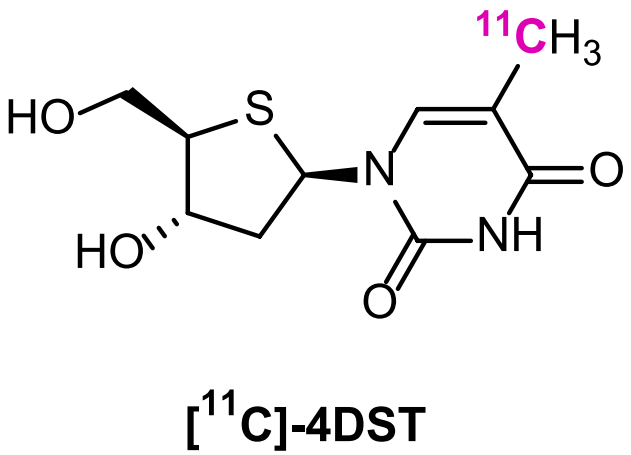


Fig. 15 Chemical structure of the cell proliferation marker [^{11}C]-4DST

have mostly relied on murine models, either using xenografts of human CRC cell lines (e.g., HT-29, HCT-116, SW620) or chemically induced tumors (e.g., azoxymethane/dextran sodium sulfate model). While xenografts offer reproducibility, they often lack a competent immune system and a realistic tumor microenvironment. HT-29 cells, for instance, show high expression of COX-2 and FAP, making them favorable for testing radiotracers such as [^{11}C]MC1 or [^{68}Ga]Ga-FAPI-04. However, other cell lines, such as HCT-116, may under-express these markers, resulting in inconsistent radiotracer uptake across studies. Furthermore, patient-derived xenograft models and orthotopic implants, though more representative, remain underutilized. Fibroblast activation protein-targeted imaging has garnered substantial interest [23–25]. Radiotracers such as [^{68}Ga]Ga-FAPI-04 and its analogs have often been associated with high tumor-to-background ratios in both animal models and early-phase clinical studies. In some reports, they appeared to outperform [^{18}F]FDG in detecting desmoplastic tumors and lesions with low glycolytic activity, such as mucinous CRC. However, quantitative variability across studies suggests that CAF abundance, tumor subtype, and imaging timing significantly impact performance. Hypoxia-targeting radiotracers such as [^{18}F]FMISO and [^{64}Cu]ATSM offer unique biological insights but face challenges in pharmacokinetics and image interpretation. While hypoxia is a known factor in CRC progression and treatment resistance, the slow washout and non-specific background signal limit widespread clinical use. Moreover, many studies use subcutaneous tumor models with limited hypoxic gradients, questioning the generalizability of preclinical results. Amino acid-based radiotracers, including [^{18}F]FET and [^{11}C]MET, have shown potential in identifying proliferative tumor regions. Yet, their utility in CRC remains less established than in neuro-oncology, owing to competing physiological uptake and variable transporter expression (e.g., LAT1, ASCT2) in colorectal tissues.

Other emerging approaches include radiolabeled vitamins and antioxidants, such as [^{68}Ga]Ga-GSH and [^{18}F]-labeled AA (ascorbic acid) analogs. These exploits altered redox metabolism in tumors but require careful interpretation because of overlapping signals from inflamed or oxidative stress-rich non-tumor tissues. Immune-PET radiotracers,

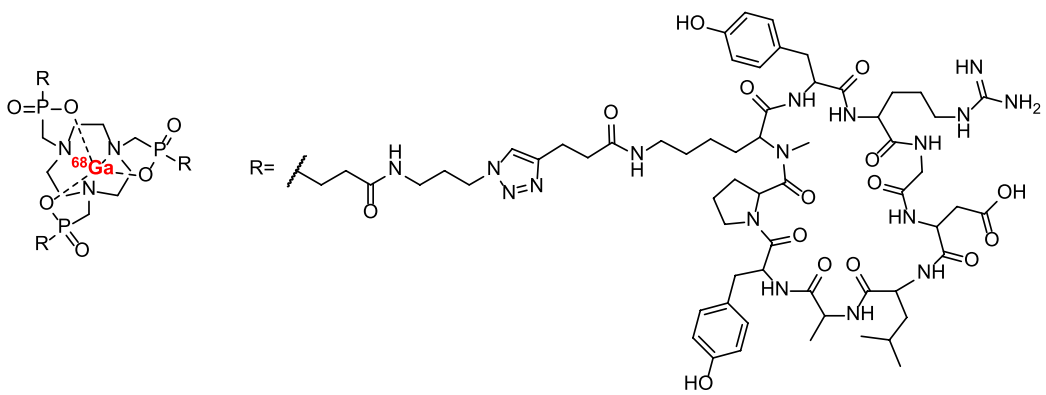


Fig. 16 Chemical structure of the integrin αvβ6 targeting[^{68}Ga]Ga-Trivehexin

Table 2 Overview of radiopharmaceuticals investigated for CRC imaging

Radiopharmaceutical	Target/biological rationale	Radionuclide and platform	Study type	CRC models used	Main imaging endpoints	Key findings	Main limitations	References
[^{18}F]DFA	SVCT2 (ascorbic acid transport)	[^{18}F] small molecule	In vitro/in vivo	SW620, HCT8 xenografts	%ID/g, T/B, 30–60 min	Tumor uptake correlated with SVCT2 expression; differentiation between CRC models	High visceral uptake; limited number of tumor models	[7]
[^{18}F]FMISO	Tumor hypoxia	[^{18}F] small molecule	In vitro/in vivo	LoVo, HT29, HCT116 xenografts	SUVmax, 4 h p.i.	Uptake correlated with hypoxia markers (HIF-1α, GLUT-1); higher uptake in LoVo	Slow clearance; high background; limited CRC-specific data	[9–16]
[^{18}F]AlF-NOTA-A6P	Integrin-α6	[^{18}F] peptide (Al^{18}F)	In vitro/in vivo	LS174T, HT29, SW620 xenografts	T/M, 60 min	High uptake in integrin-α6-positive tumors; specificity confirmed by blocking	Restricted to selected cell lines; preclinical only	[18]
[^{18}F]FB-IL-2	IL-2 receptor (immune activation)	[^{18}F] protein	In vitro/in vivo	MC38, CT26 murine tumors	Dynamic PET, biodistribution	Discriminates tumors with different immunogenic profiles	Murine models only; renal clearance	[19]
[^{68}Ga] Ga-DOTA-C21	Curcumin pathway	[^{68}Ga] small molecule	In vitro/in vivo	HT29 xenografts	T/M over time	Tumor uptake observed; improved stability vs earlier analogs	High liver and intestinal uptake; limited specificity	[20, 21]
[^{68}Ga]Ga-GSH	Glutathione metabolism	[^{68}Ga] small molecule	In vivo	DMH-induced rat CRC model	Tumor/colon ratio, 90 min	Increased uptake in tumor tissue vs normal colon	High renal/bladder uptake; limited translational data	[22]
[^{68}Ga]Ga-DOTA.SA.FAPi	FAP	[^{68}Ga] peptide	In vivo	HT29 xenografts	T/M, T/B, 1 h	High tumor contrast; favorable pharmacokinetics	Heterogeneous FAP expression; possible off-target uptake	[32]
[^{68}Ga]Ga-Pentixafor	CXCR4	[^{68}Ga] peptide	In vitro/in vivo	HT29, HCT116; CAM model	Uptake, blocking studies	Specific uptake in CXCR4-positive tumors	Limited CRC datasets; preclinical	[33]
[^{68}Ga]Ga-ES-02	HER-2	[^{68}Ga] peptide	In vitro/in vivo	HT29 xenografts	SUVmax/SUVmean, 30 min	Higher affinity and uptake vs linear analogue	HER-2 expression variability in CRC	[34–37]
[^{68}Ga]Ga-DN68	Nectin-4	[^{68}Ga] peptide	In vivo	MC38-Nectin-4 tumors	T/B, 30 min	Rapid tumor visualization; high contrast	Low Nectin-4 expression in most mCRC	[38–40]

Table 2 (continued)

Radiopharmaceutical	Target/biological rationale	Radionuclide and platform	Study type	CRC models used	Main imaging endpoints	Key findings	Main limitations	References
[^{11}C]MC1	COX-2 (inflammation)	[^{11}C] small molecule	In vivo	HT29, HCT116 xenografts	T/M, 60 min	Selective uptake in COX-2-positive tumors	Short half-life; cyclotron required	[44]
[^{64}Cu]-Tz-NOTA/SarAr	A33 antigen (pre-targeting)	[^{64}Cu] pre-targeted system	In vivo/clinical (phase I ongoing)	SW1222 xenografts; patients	T/B, T/M, 1–24 h	High tumor contrast; improved clearance with SarAr	Complex protocol; GI clearance issues	[48–50]
[^{68}Ga]Ga-HNI01	CEA	[^{68}Ga] nanobody	Preclinical/clinical (phase I, $n = 9$)	LS174T xenografts; patients with CRC	SUV, early imaging	High sensitivity for small metastases; fast kinetics	Renal uptake; small cohort	[51]
[^{68}Ga]Ga-FAPI-04	FAP	[^{68}Ga] small molecule	Clinical	CRC lesions (prospective/retrospective)	T/B, lesion detection	Superior specificity vs FDG; low false positives	Inflammation-related uptake; heterogeneity	[29, 52, 53]
[^{11}C]-4DST	Cell proliferation (DNA synthesis)	[^{11}C] nucleoside	Clinical	Patients with CRC ($n = 18$)	SUVmax	Detects CRC but lower uptake than FDG	Lower sensitivity; short half-life	[56, 57]
[^{68}Ga]Ga-Trivehexin	Integrin αvβ6	[^{68}Ga] peptide	Clinical (exploratory)	Single CRC case	SUVmax	Uptake observed in CRC lesion	Limited CRC data; preliminary	[58, 59]

CAM chorioallantoic membrane, *CEA* carcinoembryonic antigen, *CRC* colorectal cancer, *COX-2* cyclo-oxygenase-2, *DMH* dimethylhydrazine, *FAP* fibroblast activation protein, *FDG* fluoro-D-glucose, *GI* gastrointestinal, *h* hours, *HER-2* human epidermal growth factor receptor 2, *%ID/g* percentage injected dose per gram, *IL* interleukin, *min* minutes, *mCRC* metastatic CRC, *PET* positron emission tomography, *p.i.* post injection, *Ref.* reference, *SUV* standardized uptake value, *SUVmax* maximum standardized uptake value, *SUVmean* mean standardized uptake value, *SVCT2* sodium-dependent vitamin C transporter, *T/B* tumor-to-blood, *T/M* tumor-to-muscle

such as anti-programmed death-ligand 1 or CD8-targeted probes, are still in early stages of development for CRC but represent a promising frontier, particularly in the context of immunotherapy. In summary, the reviewed radiotracers illustrate the growing diversity of functional imaging strategies for CRC. Nonetheless, most studies suffer from a lack of standardized protocols, inconsistent model selection, and insufficient validation in human subjects. Direct comparative studies, ideally including head-to-head imaging with multiple radiotracers in the same model or patient, are crucial to determine real clinical utility. As CRC is a highly heterogeneous disease, both at the molecular and histological levels, future radiotracer development must consider tumor subtype, microenvironmental context, and intended clinical application (diagnosis, staging, response monitoring). Clinical studies investigating the performance of these radiotracers in human patients are still relatively limited but provide important insights. In initial clinical cohorts, [^{68}Ga]Ga-FAPI radiotracers have been reported to achieve high lesion conspicuity and, in certain CRC subtypes, higher tumor-to-background ratios compared with [^{18}F]FDG. These early data suggest that FAPI imaging may improve detection of peritoneal and liver metastases, particularly in mucinous and desmoplastic tumors where [^{18}F]FDG can be less sensitive. Likewise, [^{11}C]MC1 has shown measurable uptake in COX-2-rich rectal cancers in early-phase clinical studies, supporting further evaluation of its potential role in patient stratification for anti-inflammatory therapies. However, several radiotracers that showed favorable performance in preclinical settings have not yet translated into robust clinical trials. Issues include poor metabolic stability, high physiological background uptake (e.g., [^{18}F]FMISO in the liver and bowel), or limited availability of the radionuclide (e.g., [^{64}Cu], [^{11}C]). Furthermore, small patient cohorts and a lack of randomized comparisons with standard imaging modalities make it difficult to assess true diagnostic and prognostic value. Clinical adoption will thus depend not only on biological rationale but also on radiotracer accessibility, reproducibility of synthesis, and compatibility with current PET infrastructure.

Looking ahead, future research should prioritize the integration of radiotracer development with cutting-edge insights into CRC biology, including immune microenvironment characterization and stromal signaling. Novel targets, such as tumor-infiltrating lymphocytes or immune checkpoint molecules, may offer both prognostic and predictive value when visualized with immune-PET probes. Moreover, hybrid radiotracers capable of dual targeting or theranostic applications represent a promising frontier, especially for precision oncology. Clinically, the transition from preclinical validation to widespread adoption requires multicenter trials, standardization of synthesis and imaging protocols, and a stronger regulatory framework for novel PET agents. Additionally, the inclusion of diverse patient populations and tumor subtypes in clinical studies will be key to ensuring generalizability. Collaborations between academic institutions, radiopharmaceutical companies, and regulatory bodies will accelerate this translation and help integrate molecular imaging more broadly into clinical decision making for patients with CRC.

6 Conclusions

The growing repertoire of PET radiopharmaceuticals for CRC may support advances in early detection, molecular characterization, and longitudinal treatment monitoring. However, a rigorous assessment of existing preclinical models and target validation methodologies underscores critical shortcomings in their translational fidelity and predictive capacity for clinical outcomes. To enhance the translational robustness of novel radiotracers, future investigations should emphasize harmonized validation frameworks employing clinically relevant in vivo models, alongside well-designed comparative clinical trials aimed at substantiating preclinical efficacy within real-world therapeutic contexts.

Funding Open access funding provided by Università degli Studi di Ferrara within the CRUI-CARE Agreement.

Declarations

Funding Open access funding was provided by Università degli Studi di Ferrara within the CRUI-CARE Agreement.

Conflicts of interest/competing interests Veronica Serena Cabitza, Pier Cesare Capponi, Irene Brusa, Fabrizio Vincenzi, Silvia Pasquini, Katia Varani, and Licia Uccelli have no conflicts of interest that are directly relevant to the content of this article. Luca Urso is an Editorial Board member of *Molecular Diagnosis and Therapy*. Luca Urso was not involved in the selection of peer reviewers for the manuscript, nor any of the subsequent editorial decisions.

Ethics approval Not applicable.

Consent to participate Not applicable.

Consent for publication Not applicable.

Availability of data and material Data sharing is not applicable to this article as no datasets were generated or analyzed during the current study

Code availability Not applicable.

Authors' contributions VSC and PCC equally contributed at the present article. Conceptualization and writing first draft: VSC, PCC, and

IB; editing and revision: SP, FV, KV, LuUr, and LiUc. All authors read and approved the final version of the manuscript.

Open Access This article is licensed under a Creative Commons Attribution-NonCommercial 4.0 International License, which permits any non-commercial use, sharing, adaptation, distribution and reproduction in any medium or format, as long as you give appropriate credit to the original author(s) and the source, provide a link to the Creative Commons licence, and indicate if changes were made. The images or other third party material in this article are included in the article's Creative Commons licence, unless indicated otherwise in a credit line to the material. If material is not included in the article's Creative Commons licence and your intended use is not permitted by statutory regulation or exceeds the permitted use, you will need to obtain permission directly from the copyright holder. To view a copy of this licence, visit http://creativecommons.org/licenses/by-nc/4.0/.

References

1. Koppula BR, Fine GC, Salem AE, Covington MF, Wiggins RH, Hoffman JM, et al. PET-CT in clinical adult oncology: III. Gastrointestinal malignancies. Cancers (Basel). 2022;14(11):2668. https://doi.org/10.3390/cancers14112668.
2. Rodríguez-Fraile M, Cózar-Santiago MP, Sabaté-Llobera A, Caresia-Aróztegui AP, Delgado Bolton RC, Orcajo-Rincon J, et al. FDG PET/CT in colorectal cancer. Rev Esp Med Nucl Imagen Mol (Engl Ed). 2020;39(1):57–66. https://doi.org/10.1016/j.remn.2019.09.009.
3. Petersen RK, Hess S, Alavi A, Høilund-Carlsen PF. Clinical impact of FDG-PET/CT on colorectal cancer staging and treatment strategy. Am J Nucl Med Mol Imaging. 2014;4(5):471–82.
4. Engel R, Kudura K, Antwi K, Denhaerynck K, Steinemann D, Wullschleger S, et al. Diagnostic accuracy and treatment benefit of PET/CT in staging of colorectal cancer compared to conventional imaging. Surg Oncol. 2024;57:102151. https://doi.org/10.1016/j.suronc.2024.102151.
5. Berger KL, Nicholson SA, Dehdashti F, Siegel BA. FDG PET evaluation of mucinous neoplasms: correlation of FDG uptake with histopathologic features. AJR Am J Roentgenol. 2000;174(4):1005–8. https://doi.org/10.2214/ajr.174.4.1741005.
6. Sarikaya I, Bloomston M, Povoski SP, Zhang J, Hall NC, Knopp MV, et al. FDG-PET scan in patients with clinically and/or radiologically suspicious colorectal cancer recurrence but normal CEA. World J Surg Oncol. 2007;5:64. https://doi.org/10.1186/1477-7819-5-64.
7. He P, Zhang B, Zou Y, Zhang Y, Zha Z, Long Y, et al. Ascorbic acid analogue 6-Deoxy-6-[(18)F]fluoro-L-ascorbic acid as a tracer for identifying human colorectal cancer with SVCT2 overexpression. Transl Oncol. 2021;14(5):101055. https://doi.org/10.1016/j.tranon.2021.101055.
8. Jung SA, Lee DH, Moon JH, Hong SW, Shin JS, Hwang IY, et al. L-Ascorbic acid can abrogate SVCT-2-dependent cetuximab resistance mediated by mutant KRAS in human colon cancer cells. Free Radic Biol Med. 2016;95:200–8. https://doi.org/10.1016/j.freeradbiomed.2016.03.009.
9. Zhang MY, Zhang RJ, Jiang HJ, Jiang H, Xu HL, Pan WB, et al. (18)F-fluoromisonidazole positron emission tomography may be applicable in the evaluation of colorectal cancer liver metastasis. Hepatobiliary Pancreat Dis Int. 2019;18(2):164–72. https://doi.org/10.1016/j.hbpd.2019.02.008.
10. Xu Z, Li XF, Zou H, Sun X, Shen B. (18)F-Fluoromisonidazole in tumor hypoxia imaging. Oncotarget. 2017;8(55):94969–79. https://doi.org/10.18632/oncotarget.21662.
11. Marcus C, Subramaniam RM. Role of non-FDG-PET/CT in head and neck cancer. Semin Nucl Med. 2021;51(1):68–78. https://doi.org/10.1053/j.semnuclmed.2020.07.008.
12. Hirata K, Yamaguchi S, Shiga T, Kuge Y, Tamaki N. The roles of hypoxia imaging using (18)F-fluoromisonidazole positron emission tomography in glioma treatment. J Clin Med. 2019;8(8):1088. https://doi.org/10.3390/jcm8081088.
13. Chen DL, Dehdashti F. Advances in positron emission tomographic imaging of lung cancer. Proc Am Thorac Soc. 2005;2(6):541–4. https://doi.org/10.1513/pats.200507-075DS.
14. Tao R, Ager B, Lloyd S, Torgeson A, Denney M, Gaffney D, et al. Hypoxia imaging in upper gastrointestinal tumors and application to radiation therapy. J Gastrointest Oncol. 2018;9(6):1044–53. https://doi.org/10.21037/jgo.2018.09.15.
15. Vallières M, Serban M, Benzyane I, Ahmed Z, Xing S, El Naqa I, et al. Investigating the role of functional imaging in the management of soft-tissue sarcomas of the extremities. Phys Imaging Radiat Oncol. 2018;6:53–60. https://doi.org/10.1016/j.phro.2018.05.003.
16. Lee ST, Tebbutt N, Gan HK, Liu Z, Sachinidis J, Pathmaraj K, et al. Evaluation of (18)F-FMISO PET and (18)F-FDG PET scans in assessing the therapeutic response of patients with metastatic colorectal cancer treated with anti-angiogenic therapy. Front Oncol. 2021;11:606210. https://doi.org/10.3389/fonc.2021.606210.
17. Niu J, Li Z. The roles of integrin αvβ6 in cancer. Cancer Lett. 2017;403:128–37. https://doi.org/10.1016/j.canlet.2017.06.012.
18. Chen L, Fu H, Li W, Shen Q, Luo Y, Fu J, et al. Development and preclinical evaluation of a cyclic PET tracer targeting integrin-α6 on colorectal cancer models. Bioorg Chem. 2024;153:107892. https://doi.org/10.1016/j.bioorg.2024.107892.
19. Khanapur S, Yong FF, Hartimath SV, Jiang L, Ramasamy B, Cheng P, et al. An improved synthesis of N-(4-[(18)F] fluorobenzoyl)-interleukin-2 for the preclinical PET imaging of tumour-infiltrating T-cells in CT26 and MC38 colon cancer models. Molecules. 2021;26(6):1728. https://doi.org/10.3390/molecules26061728.
20. Orteca G, Pisaneschi F, Rubagotti S, Liu TW, Biagiotti G, Piwnica-Worms D, et al. Development of a potential gallium-68-labelled radiotracer based on DOTA-curcumin for colorectal carcinoma: from synthesis to in vivo studies. Molecules. 2019;24(3):644. https://doi.org/10.3390/molecules24030644.
21. Rubagotti S, Croci S, Ferrari E, Orteca G, Iori M, Capponi PC, et al. Uptake of Ga-curcumin derivatives in different cancer cell lines: toward the development of new potential (68)Ga-labelled curcuminoids-based radiotracers for tumour imaging. J Inorg Biochem. 2017;173:113–9. https://doi.org/10.1016/j.jinorgbio.2017.05.002.
22. Sidiq S, Dhawan DK, Kumar RR, Shukla J, Mittal BR, Chadha VD. (68)Ga-glutathione radio-complex as a new diagnostic probe for targeting colon cancer in rats. Hell J Nucl Med. 2019;22(2):131–4. https://doi.org/10.1967/s002449911006.
23. Mori Y, Dendl K, Cardinale J, Kratochwil C, Giesel FL, Haberkorn U. FAPI PET: fibroblast activation protein inhibitor use in oncologic and nononcologic disease. Radiology. 2023;306(2):e220749. https://doi.org/10.1148/radiol.220749.
24. Boschi A, Urso L, Uccelli L, Martini P, Filippi L. (99m)Tc-labeled FAPI compounds for cancer and inflammation: from radiochemistry to the first clinical applications. EJNMMI Radiopharm Chem. 2024;9(1):36. https://doi.org/10.1186/s41181-024-00264-0.
25. Ortolan N, Urso L, Zamberlan I, Filippi L, Buffi NM, Cittanti C, et al. Is there a role for FAPI PET in urological cancers? Mol Diagn Ther. 2024;28(6):721–5. https://doi.org/10.1007/s40291-024-00735-9.
26. Selcuk NA, Beydagi G, Akcay K, Gormez A, Toklu T, Kabasakal L. The role of [68Ga]Ga-FAP-2286 PET/CT in the evaluation of

treatment response in gastrointestinal system malignancies. Eur J Nucl Med Mol Imaging. 2026;53(3):1491–7. https://doi.org/10.1007/s00259-025-07597-1.
27. Xi Y, Sun Y, Gu B, Bian L, Song S. Evaluation of (68)Ga-FAPI PET/CT and (18)F-FDG PET/CT for the diagnosis of recurrent colorectal cancers. Clin Transl Radiat Oncol. 2024;49:100848. https://doi.org/10.1016/j.ctro.2024.100848.
28. Lin X, Li Y, Wang S, Zhang Y, Chen X, Wei M, et al. Diagnostic value of [(68)Ga]Ga-FAPI-04 in patients with colorectal cancer in comparison with [(18)F]F-FDG PET/CT. Front Oncol. 2022;12:1087792. https://doi.org/10.3389/fonc.2022.1087792.
29. Kömek H, Can C, Kaplan İ, Gündoğan C, Kepenek F, Karaoglan H, et al. Comparison of [(68)Ga]Ga-DOTA-FAPI-04 PET/CT and [(18)F]FDG PET/CT in colorectal cancer. Eur J Nucl Med Mol Imaging. 2022;49(11):3898–909. https://doi.org/10.1007/s00259-022-05839-0.
30. Alan Selçuk N, Beydağı G, Akçay K, Demirci E, Görmez A, Öven BB, et al. Impact of (68)Ga-FAPi PET/CT on staging or restaging digestive system tumors in patients with negative or equivocal (18)F-FDG PET/CT findings. Mol Imaging Radionucl Ther. 2025;34(1):31–7. https://doi.org/10.4274/mirt.galenos.2024.50470.
31. Polack M, van Pelt GW, Crobach A, de Geus-Oei LF, Tollenaar R, van Krieken J, et al. Fibroblast activation protein-expression in colorectal carcinomas and implications for clinical application. Cancer Treat Res Commun. 2025;44:100964. https://doi.org/10.1016/j.ctarc.2025.100964.
32. Moon ES, Elvas F, Vliegen G, De Lombaerde S, Vangestel C, De Bruycker S, et al. Targeting fibroblast activation protein (FAP): next generation PET radiotracers using squaramide coupled bifunctional DOTA and DATA(5m) chelators. EJNMMI Radiopharm Chem. 2020;5(1):19. https://doi.org/10.1186/s41181-020-00102-z.
33. Benčurová K, Friske J, Anderla M, Mayrhofer M, Wanek T, Nics L, et al. CAM-xenograft model provides preclinical evidence for the applicability of [(68)Ga]Ga-Pentixafor in CRC imaging. Cancers (Basel). 2022;14(22):5549. https://doi.org/10.3390/cancers14225549.
34. Richman SD, Southward K, Chambers P, Cross D, Barrett J, Hemmings G, et al. HER2 overexpression and amplification as a potential therapeutic target in colorectal cancer: analysis of 3256 patients enrolled in the QUASAR, FOCUS and PICCOLO colorectal cancer trials. J Pathol. 2016;238(4):562–70. https://doi.org/10.1002/path.4679.
35. Siena S, Sartore-Bianchi A, Marsoni S, Hurwitz HI, McCall SJ, Penault-Llorca F, et al. Targeting the human epidermal growth factor receptor 2 (HER2) oncogene in colorectal cancer. Ann Oncol. 2018;29(5):1108–19. https://doi.org/10.1093/annonc/mdy100.
36. Khelwatty SA, Essapen S, Bagwan I, Green M, Seddon AM, Modjtahedi H. Co-expression of HER family members in patients with Dukes' C and D colon cancer and their impacts on patient prognosis and survival. PLoS ONE. 2014;9(3):e91139. https://doi.org/10.1371/journal.pone.0091139.
37. Zhang J, Lin Y, Gao J, Pan Y, Hou G, Guo C, et al. Development and biological evaluation of (68)Ga-labeled peptides for potential application in HER2-positive colorectal cancer. Bioorg Chem. 2024;151:107645. https://doi.org/10.1016/j.bioorg.2024.107645.
38. Speltri G, Badrane I, Napolitano R, Boschi A, Uccelli L, Filippi L, et al. Nectin-4-targeting radiotracers: novel theranostic agents for precision oncology in cancer. Mol Diagn Ther. 2025;29(4):453–63. https://doi.org/10.1007/s40291-025-00786-6.
39. Moretto R, Germani MM, Giordano M, Conca V, Proietti A, Niccoli C, et al. Trop-2 and Nectin-4 immunohistochemical expression in metastatic colorectal cancer: searching for the right population for drugs' development. Br J Cancer. 2023;128(7):1391–9. https://doi.org/10.1038/s41416-023-02180-7.
40. Ge S, Jia T, Shi J, Cao J, Sang S, Li J, et al. A cutting-edge (68)Ga-labeled bicyclic peptide PET molecular probe for non-invasive assessment of Nectin4 expression. Bioorg Chem. 2024;152:107745. https://doi.org/10.1016/j.bioorg.2024.107745.
41. Hashemi Goradel N, Najafi M, Salehi E, Farhood B, Mortezaee K. Cyclooxygenase-2 in cancer: a review. J Cell Physiol. 2019;234(5):5683–99. https://doi.org/10.1002/jcp.27411.
42. Sheng J, Sun H, Yu FB, Li B, Zhang Y, Zhu YT. The role of cyclooxygenase-2 in colorectal cancer. Int J Med Sci. 2020;17(8):1095–101. https://doi.org/10.7150/ijms.44439.
43. Ogino S, Kirkner GJ, Nosho K, Irahara N, Kure S, Shima K, et al. Cyclooxygenase-2 expression is an independent predictor of poor prognosis in colon cancer. Clin Cancer Res. 2008;14(24):8221–7. https://doi.org/10.1158/1078-0432.CCR-08-1841.
44. Boyle AJ, Narvaez A, Tong J, Zoghbi SS, Pike VW, Innis RB, et al. Repurposing [(11)C]MC1 for PET imaging of cyclooxygenase-2 in colorectal cancer xenograft mouse models. Mol Imaging Biol. 2022;24(3):365–70. https://doi.org/10.1007/s11307-021-01675-0.
45. Altai M, Membreno R, Cook B, Tolmachev V, Zeglis BM. Pretargeted imaging and therapy. J Nucl Med. 2017;58(10):1553–9. https://doi.org/10.2967/jnumed.117.189944.
46. García-Vázquez R, Battisti UM, Herth MM. Recent advances in the development of tetrazine ligation tools for pretargeted nuclear imaging. Pharmaceuticals (Basel). 2022;15(6):685. https://doi.org/10.3390/ph15060685.
47. Qiu L, Mao W, Yin H, Tan H, Cheng D, Shi H. Pretargeted nuclear imaging and radioimmunotherapy based on the inverse electron-demand Diels-Alder reaction and key factors in the pretargeted synthetic design. Contrast Media Mol Imaging. 2019;2019:9182476. https://doi.org/10.1155/2019/9182476.
48. Zeglis BM, Sevak KK, Reiner T, Mohindra P, Carlin SD, Zanzonico P, et al. A pretargeted PET imaging strategy based on bioorthogonal Diels-Alder click chemistry. J Nucl Med. 2013;54(8):1389–96. https://doi.org/10.2967/jnumed.112.115840.
49. Zeglis BM, Brand C, Abdel-Atti D, Carnazza KE, Cook BE, Carlin S, et al. Optimization of a pretargeted strategy for the PET imaging of colorectal carcinoma via the modulation of radioligand pharmacokinetics. Mol Pharm. 2015;12(10):3575–87. https://doi.org/10.1021/acs.molpharmaceut.5b00294.
50. Cook BE, Adumeau P, Membreno R, Carnazza KE, Brand C, Reiner T, et al. Pretargeted PET imaging using a site-specifically labeled immunoconjugate. Bioconjug Chem. 2016;27(8):1789–95. https://doi.org/10.1021/acs.bioconjchem.6b00235.
51. Li L, Lin X, Wang L, Ma X, Zeng Z, Liu F, et al. Immuno-PET of colorectal cancer with a CEA-targeted [68Ga]Ga-nanobody: from bench to bedside. Eur J Nucl Med Mol Imaging. 2023;50(12):3735–49. https://doi.org/10.1007/s00259-023-06313-1.
52. Pang Y, Zhao L, Luo Z, Hao B, Wu H, Lin Q, et al. Comparison of (68)Ga-FAPI and (18)F-FDG uptake in gastric, duodenal, and colorectal cancers. Radiology. 2021;298(2):393–402. https://doi.org/10.1148/radiol.2020203275.
53. Shangguan C, Yang C, Shi Z, Miao Y, Hai W, Shen Y, et al. (68)Ga-FAPI-04 positron emission tomography distinguishes malignancy from (18)F-FDG-avid colorectal lesions. Int J Radiat Oncol Biol Phys. 2024;118(1):285–94. https://doi.org/10.1016/j.ijrobp.2023.08.019.
54. García Megías I, Almeida LS, Calapaquí Terán AK, Pabst KM, Herrmann K, Giammarile F, et al. FAPI radiopharmaceuticals in nuclear oncology and theranostics of solid tumours: are we nearer to surrounding the hallmarks of cancer? Ann Nucl Med. 2025;39(5):407–23. https://doi.org/10.1007/s12149-025-02022-x.

55. Toyohara J, Okada M, Toramatsu C, Suzuki K, Irie T. Feasibility studies of 4'-[methyl-(11)C]thiothymidine as a tumor proliferation imaging agent in mice. Nucl Med Biol. 2008;35(1):67–74. https://doi.org/10.1016/j.nucmedbio.2007.10.001.
56. Toyohara J, Nariai T, Sakata M, Oda K, Ishii K, Kawabe T, et al. Whole-body distribution and brain tumor imaging with (11)C-4DST: a pilot study. J Nucl Med. 2011;52(8):1322–8. https://doi.org/10.2967/jnumed.111.088435.
57. Fukuda Y, Yamamoto Y, Mitamura K, Ishikawa R, Asano E, Toyohara J, et al. 4'-[methyl-(11)C]-thiothymidine as a proliferation imaging tracer for detection of colorectal cancer: comparison with (18)F-FDG. Ann Nucl Med. 2019;33(11):822–7. https://doi.org/10.1007/s12149-019-01393-2.
58. Costa A, Silvestrini R, Mochen C, Lequaglie C, Boracchi P, Faranda A, et al. P53 expression, DNA ploidy and S-phase cell fraction in operable locally advanced non-small-cell lung cancer. Br J Cancer. 1996;73(7):914–9. https://doi.org/10.1038/bjc.1996.163.
59. Urso L, Napolitano R, Speltri G, Tuncel M, Badrane I, Uccelli L, et al. (68)Ga-Trivehexin: current status of αvβ6-integrin imaging and perspectives. Cancers (Basel). 2025;17(9):1504. https://doi.org/10.3390/cancers17091504.
60. Das SS, Ahlawat S, Thakral P, Malik D, Simecek J, Virupakshappa CB, et al. Potential efficacy of 68 Ga-Trivehexin PET/CT and immunohistochemical validation of αvβ6 integrin expression in patients with head and neck squamous cell carcinoma and pancreatic ductal adenocarcinoma. Clin Nucl Med. 2024;49(8):733–40. https://doi.org/10.1097/RLU.0000000000005278.